

Application of Supercapacitor for Braking Energy Recovery in Electric Bicycles

By

Enrico Catahan

*Thesis
Submitted to Flinders University
for the degree of*

Master of Engineering (Electrical and Electronics)

College of Science and Engineering
June 2024

TABLE OF CONTENTS

TABLE OF CONTENTS	I
ABSTRACT	III
DECLARATION	IV
ACKNOWLEDGEMENTS	V
LIST OF FIGURES	VI
LIST OF TABLES	VIII
1. INTRODUCTION	1
1.1. Background	1
1.2. Summary of literature	2
1.3. Objectives.....	2
1.4. Scope and Limitations	3
1.5. Methods	3
1.6. Outline of the thesis.....	3
2. LITERATURE REVIEW	4
2.1. The e-bike model.....	4
2.2. Power requirements	4
2.3. Power management	5
2.4. Methods of power conversion	6
2.5. Testing approach.....	8
2.5.1. Prototype testing.....	8
2.5.2. Simulation model	10
2.6. Gap statement.....	11
2.7. Contribution	11
3. METHODOLOGY	12
3.1. Introduction.....	12
3.2. Determining of parameters	12
3.2.1. BLDC motor	12
3.2.2. Torque load	13
3.2.3. Brake load	13
3.2.4. Manual pedal input	14
3.2.5. Drive cycle	15
3.2.6. Battery and supercapacitor	16
3.3. System model.....	16
3.3.1. Conventional e-bike model.....	16
3.3.2. Proposed regenerative braking system model	17
3.4. Limitations	17
3.4.1. Data memory and sampling time.....	17
4. RESULTS AND ANALYSIS	18

4.1.	Introduction.....	18
4.2.	Battery discharge response	18
4.3.	Supercapacitor discharging	18
4.3.1.	Discharge characteristics during acceleration	18
4.4.	Supercapacitor charging characteristics	19
4.4.1.	Charge vs. road slope.....	19
4.4.2.	Charge vs. braking distance.....	20
4.5.	Drive cycle application.....	21
4.5.1.	Battery discharge rate.....	21
4.5.2.	Supercapacitor utilisation.....	22
4.6.	Cost comparison.....	23
5.	CONCLUSIONS AND FUTURE WORK	24
5.1.	Conclusions.....	24
5.2.	Future Work.....	25
5.2.1.	Determination of optimum riding conditions	25
5.2.2.	Improvement of charging efficiency.....	25
5.2.3.	Obtaining more routes and drive cycle data	25
5.2.4.	Prototype build and test	25
	BIBLIOGRAPHY	26
	APPENDIX A: ANSYS RMXprt PARAMETERS	31
	APPENDIX B: SIMULATION MODEL BLOCKS	34


ABSTRACT

In a generation where the consequences of climate change have become more apparent, environmental awareness has been rapidly gaining momentum. There has been more conscious effort to promote sustainability and reduce carbon footprints. The transportation sector is one of the major culprits of CO₂ emissions worldwide. The development of green transportation has been crucial to sustainable mobility as operating one does not produce carbon emissions. Electric bicycles, whose popularity worldwide continues to rise, requires minimal space, and contributes to reducing traffic. But comparing to electric vehicles (EVs), e-bikes have much smaller batteries, which translates to a significantly shorter driving range. While battery technology continues to develop, it still generally suffers from a limited lifespan. Regenerative braking, which converts kinetic energy produced by a moving body to electrical energy, is almost synonymous to EVs. Due to the significant difference in weight and driving speed limitations, e-bikes have much less kinetic energy potential compared to EVs. This study proposes a regenerative braking system for e-bikes that utilises the high power density of supercapacitors to more efficiently store energy recovered during braking. The improvement in the motor drive range compared to a conventional e-bike was investigated using simulation models developed in MATLAB/Simulink. Charging and discharging characteristics of the supercapacitor were measured with changes to the road inclination and braking behaviour and a drive cycle representing an actual bicycle route in South Australia was derived to obtain a practical representation of the improvement in performance. The results of the study showed the potential of regenerative braking in e-bikes using supercapacitors and discusses the conditions that need to be met for effective energy recovery during braking. Future plans suggest the next steps in the study, including which factors to focus on to maximize energy recovery.

DECLARATION

I certify that this thesis:

1. does not incorporate without acknowledgment any material previously submitted for a degree or diploma in any university.
2. and the research within will not be submitted for any other future degree or diploma without the permission of Flinders University; and
3. to the best of my knowledge and belief, does not contain any material previously published or written by another person except where due reference is made in the text.

Signature of student.....

Print name of student..... Enrico Catahan.....

Date..... 29/6/2024.....

I certify that I have read this thesis. In my opinion it is/is not (please circle) fully adequate, in scope and in quality, as a thesis for the degree of Master of Engineering (Electronics and Electrical). Furthermore, I confirm that I have provided feedback on this thesis and the student has implemented it minimally/partially/fully (please circle).

Signature of Principal Supervisor.....

Print name of Principal Supervisor.....

Date.....

ACKNOWLEDGEMENTS

Firstly, I would like to acknowledge Dr. Amin Mahmoudi for this project, the continuous support, and most of all, accepting to supervise me, even if I was not in any of your topics.

I am also acknowledging Bingjian Li and Zhi Cao for providing me with very useful insights and suggestions, particularly when I was still starting out with this project.

I would like to thank my parents for the encouraging words and emotional support even when I am 2,700 miles away from home.

And most of all, I am very thankful for my wife, Manna, for being patient and understanding, and continuously working hard so that I can concentrate on my studies.

LIST OF FIGURES

Figure 1. Basic block diagram of an electric bicycle (Sathiyar <i>et al.</i> 2018).....	4
Figure 2. Forces in a bicycle moving uphill (Contò and Bianchi 2023].....	4
Figure 3. Model of transmission system using a mid-drive motor (Balaji <i>et al.</i> 2011).....	7
Figure 4. Non-isolated half-bridge bidirectional DC-DC converter (Sharma <i>et al.</i> 2018).....	7
Figure 5. Timing diagram for three-phase motor line voltages (Morchin and Oman 2006).....	8
Figure 6. Three-phase bridge rectifier (Rashid 2014).	8
Figure 7. Current of battery and supercapacitor when starting the motor (Karandikar 2012).	9
Figure 8. 3D model of the outer rotor BLDC motor used in this study.....	12
Figure 9. Dimensions for a 26" bicycle wheel (bikegremlin.com 2024).	13
Figure 10. Cycling route used in the drive cycle.	15
Figure 11. Changes in road elevation at various points of the cycling route.	15
Figure 12. System block diagram of the conventional e-bike model.	16
Figure 13. System block diagram of the proposed regenerative braking model.....	17
Figure 14. Battery discharge and torque load/current plots for one acceleration-brake cycle.	18
Figure 15. Plot of supercapacitor charge vs. speed and time.	20
Figure 16. Plot of battery charge at the end of each drive cycle section.	21
Figure 17. Charge of supercapacitor at the end of each section.....	22
Figure 18. Supercapacitor energy at various points in time.	22
Figure 19. Machine general parameters.....	31
Figure 20. Drive circuit parameters.	31
Figure 21. Stator general parameters.....	31
Figure 22. Stator slot dimensions.....	32
Figure 23. Stator winding parameters.	32
Figure 24. Rotor general parameters.	32
Figure 25. Rotor pole parameters.	33
Figure 26. Shaft parameters.	33
Figure 27. Analysis setup parameters.....	33
Figure 28. Top-level of Simulink model of Regenerative Braking System.....	34
Figure 29. Three-phase power inverter block.	35
Figure 30. Commutation logic block.	36
Figure 31. Movement and load status block.	37
Figure 32. Torque load calculation block.....	38
Figure 33. Accelerate/Brake/Regen control block.....	39
Figure 34. Manual pedal input control block.	40
Figure 35. Buck converter block.....	41
Figure 36. Boost converter block.....	42
Figure 37. Buck/Boost mode select.....	42
Figure 38. Drive source selection block.....	43
Figure 39. Torque brake controller block.....	44

Figure 40. Three-phase bridge rectifier. 45
Figure 41. Electronic brake controller. 45

LIST OF TABLES

Table 1. Summary of existing works on electric bicycle regenerative braking.....	2
Table 2. E-bike and load parameters	13
Table 3. Parameter for torque braking.....	14
Table 4. Parameters for manual pedal input.....	14
Table 5. Drive cycle and riding behaviour parameters used in the test.....	14
Table 6. Charge of 30F 27V supercapacitor bank after acceleration phase.....	19
Table 7. Charge of 15F 27V supercapacitor bank after acceleration phase.....	19
Table 8. Supercapacitor charge after 1 cycle.	19
Table 9. Supercapacitor charge compared to braking distance (slope = 0°).	20
Table 10. Battery and supercapacitor charge status at various sections of the drive cycle.....	21
Table 11. Option 1: Battery upgrade (20% increase in capacity).....	23
Table 12. Option 2: Regenerative braking with supercapacitors.....	23

1. INTRODUCTION

1.1. Background

The popularity of electric bicycles has continuously grown worldwide, more so in recent years. Countries with strong bicycle culture, such as Japan and China, have long had strong e-bike sales (Roshan *et al.* 2021). Even though the bicycle came from western origins, local empowerment in these countries had made the bicycle had become more associated with Asia. The surging market for e-bikes has benefited from the new fashion for bicycle commuting, a well-developed cycling infrastructure, and bike-sharing schemes in various parts of the world (Smethurst 2015).

Taking a quick look at history, Japan was the first country in Asia to have a significant local bicycle industry, soon to follow was China and India. The e-bike, the next step in the technological development of bicycles, is considered by some to eventually displace the fully pedal-driven bicycles. By 2015, the Chinese e-bike industry has become the majority producer the world, reaching a production volume of 20 million units a year, in the year where the global industry was worth USD11 billion. Currently, Asian factories continue to produce e-bikes both for the west and for local consumers (Smethurst 2015). Led by European countries, such as Germany, there has been a significant shift towards e-bikes by consumers as an alternative mode of transportation to the also environmentally-friendly Electric Vehicles (EVs) (Deloitte.com 2022).

Cycling has been known to improve general fitness but poses a challenge for those with physical limitations. The pedal-assist of e-bikes makes the uphill climbs easier, which can encourage people to take up cycling (businessinsider.com 2023). But e-bikes also have definite disadvantages in comparison to EVs. Due to its construction and weight considerations, the battery size becomes limited, resulting in a significantly lower riding range and short battery lifespan (He 2022; Hatwar *et al.* 2013; Sharma *et al.* 2018).

There are also legal limitations in the ownership and usage of e-bikes. In South Australia, it is not required to obtain a driver's license to operate a road legal e-bike (SA.gov.au 2023). The road legal e-bike in Australia, and in other countries such as the UK, must comply with the European Committee for Standardization EN 15194:2009 or EN 15194:009+A1:2011 Cycles – Electrically power assisted cycles – EPAC Bicycle ('EN15194'). As included in this standard, the motor must be electric and not exceed a continuous output power of 250W. The power of the motor should also cut-off once the speed reaches 25km/h. The rider may still go beyond the speed limit, depending on local road regulations, but on manual pedal alone. The rider must also pedal to activate the e-bike's pedal-assist, unless the speed is below 6km/h. Exceeding the power rating or having an internal combustion engine classifies the transportation as a vehicle and operating requires a valid driver's license (SA.gov.au 2023; police.sa.gov.au n.d.).

Electric vehicles (EVs) typically have shorter range than its internal combustion (IC) engine counterpart. Along with improvements in battery technology, the introduction of regenerative braking has significantly improved the EV's range. Regenerative braking is a technique for recovering part of the kinetic energy normally lost due to friction during braking. During braking, the torque is used to charge the battery (Nain *et al.* 2021; Permana *et al.* 2018).

In addition to improving battery range, regenerative braking also reduces reliance on frictional brakes, therefore extending its service life. But frictional brakes are still necessary to be used in conjunction with regenerative braking, particularly at low speeds and bringing the vehicle to a complete stop. For light transportation, such as e-bikes, one of the concerns with regenerative braking is the significantly lower kinetic energy compared to EV's due to the disparity in mass. A car can have 160 times the kinetic energy that of a bicycle (Vasiljević *et al.* 2022; Balaji *et al.* 2010; Karandikar *et al.* 2012; Morchin and Oman 2006).

Therefore, to implement an effective regenerative braking for e-bikes, an efficient method of storing recovered energy needs to be investigated.

1.2. Summary of literature

There are currently only limited studies about regenerative braking in e-bikes. There are even a few that have considered using supercapacitors for energy recovery storage. Table 1 below summarises the existing works that is discussed in the literature review section of this paper.

Table 1. Summary of existing works on electric bicycle regenerative braking.

Ref.	Author	Regenerative Braking circuit	Supercapacitor application	Simulation/ Prototype	Driving behaviour	Maximum test speed
[1]	Balaji <i>et al.</i>	Diodes and electronic switches	N/A (Battery only)	Prototype	Fixed speed per test	45km/h
[2]	Karandikar <i>et al.</i>	Alternator with rectifier	Assist battery in starting the motor	Prototype	Actual road test	21km/h
[3]	Malan <i>et al.</i>	Bidirectional DC-DC converter	Main power source	Prototype	Actual road test	20km/h
[4]	Permana <i>et al.</i>	Bidirectional DC-DC converter	Assist battery in starting the motor	Simulation (PSIM)	NYCC drive cycle	45km/h
[5]	Ilahi <i>et al.</i>	Bidirectional DC-DC converter	N/A (Battery only)	Simulation (Multisim)	Maximum speed only	50km/h
[6]	Sreehari <i>et al.</i>	Boost converter	N/A (Battery only)	Prototype	Fixed speed per test	25km/h
[7]	Roshan <i>et al.</i>	Bidirectional DC-DC converter	N/A (Battery only)	Prototype	Fixed speed per test	52km/h
[8]	Naveed <i>et al.</i>	3-Phase rectifier with variable load	Not mentioned in paper	Prototype	Fixed speed per test	25km/h

1.3. Objectives

1. To propose a concept and simulate a regenerative braking system for an electric bicycle using supercapacitors.
2. To analyse the improvement technically and economically in the pedal-assist range with a designed riding course.

1.4. Scope and Limitations

The scope of this project includes the creation of a simulation model of the propulsion and brake control of a road legal electric bicycle. This includes creation of an energy management algorithm that shifts the power source of the e-bike between a lithium-ion battery and a supercapacitor bank for the system with regenerative braking. Additionally, a drive cycle is designed based on an actual cycling route in South Australia and is used as the input variable to the simulation models.

The project's focus is on determining the potential amount of energy recovery theoretically, and a build of an actual prototype is not included in the scope. Also, since there are no publicly available data for the road conditions, the road constants and coefficients will be based on typical data from previous studies. Effects to the lifecycle of the battery and supercapacitor are also not considered in the analysis of results.

1.5. Methods

The focus of this project was to determine the improvement in the range of the e-bike pedal assist with the application of the proposed regenerative braking system using supercapacitors.

Simulation models for a conventional e-bike and with the proposed regenerative braking were created using MATLAB/Simulink, while the three-phase BLDC motor was designed using ANSYS Maxwell software. Battery discharging and supercapacitor charging/discharging performance with respect to road conditions and riding behaviour were compared. The primary data used for the conclusion of the study is the State of Discharge (SoD) of the battery at the end of the designed drive cycle, which is used to determine the pedal-assist range for both cases.

1.6. Outline of the thesis

This manuscript is composed of 5 major chapters, which are further divided into multiple sections. Chapter 1 briefly introduces the current status of e-bikes, limitations, and how this project plans to address those limitations. Chapter 2 provides insights on the available text regarding works on regenerative braking for e-bikes and determines an approach that would further knowledge on the subject. Chapter 3 details the steps done in the analysis, including the determination of parameters that were used in the build of the simulation models and limitations. Chapter 4 provides the results of the simulations performed in MATLAB/Simulink and discusses the parameters that affect regenerative braking. The overall improvement in the driving range with the derived drive cycle is also determined in this section. The final chapter ties up the study with the conclusion and suggestions for future activities regarding the subject.

2. LITERATURE REVIEW

2.1. The e-bike model

The basic electric bicycle consists of a motor, transmission, a power converter, a controller, and a battery installed in a bicycle. The battery provides the energy to the motor for propulsion, but to control the rotational speed, it goes through a power electronic converter, which is a three-phase power inverter for three-phase BLDC motors. The transmission transmits power from the motor and the pedal to the wheel. The controller ties up all the functions by receiving information from the user (assist level), the wheel (speed), and battery (charge level), then controls the power converter to regulate the output voltage to the motor (Sathiyar *et al* 2018). Figure 1 shows the basic block diagram of an e-bike as described above. The battery, power converter, motor, and controller are the four blocks primarily involved in application of regenerative braking.

Removed due to copyright restrictions.

Figure 1. Basic block diagram of an electric bicycle (Sathiyar *et al.* 2018).

2.2. Power requirements

Generating movement on an e-bike going uphill requires power to overcome wind resistance, lifting mass up a hill, and bearings and tire friction [1][51] [47]. Figure 2 shows how propulsion and resistive forces relate to each other. Various studies used different naming conventions for the forces involved, but the concepts are all the same (Morchin and Owen 2006; Muetze *et al.* 2005; Contò and Bianchi 2023).

Removed due to copyright restrictions.

Figure 2. Forces in a bicycle moving uphill (Contò and Bianchi 2023).

The power consumption P_{tot} is equal to the sum of the power to overcome wind resistance P_{drag} , lifting a mass uphill P_{hill} , and overcoming frictions $P_{friction}$:

$$P_{tot} = P_{drag} + P_{hill} + P_{friction} \quad (1)$$

The power required to climb a hill is the product of the vertical force due to the total mass of the e-bike and rider (N) and the ground speed v_g (m/s²), where:

$$P_{hill} = mgv_g \sin \alpha [W] \quad (2)$$

The power required to overcome wind drag is determined in terms of the drag coefficient C_d , air density ρ_{air} , surface area normal to the riding direction A , ground speed and wind velocity vector v_w . v_w is a positive value if the wind direction opposes the riding direction, and negative if it aids the rider.

$$P_{drag} = \frac{1}{2} C_d \rho_{air} A (v_g + v_w)^2 v_g [W] \quad (3)$$

The power required to overcome rolling resistance due to friction is calculated using equation 4 below where C_{rr} represents the coefficient of rolling resistance.

$$P_{friction} = mgC_{rr}v_g \cos \alpha \quad (4)$$

Since power is equal to force times the velocity of an object, removing the ground speed leaves the force of wind resistance F_{drag} as the only force dependent on speed. The total load torque is then equal to the sum of the forces multiplied by the radius r of the wheel.

While the calculations above determine the forces needed to be overcome for propulsion, Morchin and Omar (2006) adds the additional force needed to propel or accelerate the e-bike to a desired speed.

$$F_a = ma \quad (5)$$

More energy is needed to increase the speed when travelling faster due to power being proportional to force and velocity. In summary, the total power required to increase the speed of the e-bike is the sum of the power to overcome gravity, wind resistance, rolling resistance, and the accelerating power.

2.3. Power management

Typical batteries of e-bikes range from 24 to 48V. Older models mostly use lead-acid and nickel-zinc, which are much heavier than lithium-ion batteries. Li-ion batteries are the most popular type

used today due to its light weight, long life, and high energy density (160 Wh/kg). In comparison, lead-acid batteries can deliver 20Wh/kg (Morchin and Omar 2006).

Majority of studies chose batteries as the main power source of their e-bike design, with various ratings due to different motors used. Sreehari M D, *et al.* (2020) used 2 12V 26Ah lead-acid batteries in series to power a 24W 350W BLDC motor. For 48V 350W motor, T.I.N Roshan, *et al.* (2021) used 48V batteries. Alternatively, Malan *et al.* (2014) powered their e-bikes using only a 36V supercapacitor bank. The limitation in the range was not a factor since the study only involved short distance travels around a campus loop. The limitation in range was able to be demonstrated by Ammayapan *et al.* (2023), whose 48V 250W e-bike prototype ran only a maximum of 2.5km with 51V 190F supercapacitors.

A third set of works, Karandikar *et al* (2012), Permana *et al* (2018), and Naveed *et al* (2022) went with the hybrid supply, combining a battery and a supercapacitor bank to provide power to the e-bike motor, though Naveed only mentioned the use, but not actually implemented in his tests. Hybrid supply takes advantage of the strengths of the power sources to improve the pedal-assist range (Dash *et al.* 2022). Batteries have high energy density but have limited lifecycle that is further degraded by frequent charge/discharge cycles. Supercapacitors store less energy but can deliver higher power and current, with a significantly faster charging time (Hatwar *et al.* 2013). Karandikar and Permana supported the theory of the battery and supercapacitor sharing power load to prolong the battery's lifespan. By configuring the supercapacitor to assist the battery during propulsion, the supercapacitor provides bulk of the initial peak currents. During regenerative braking, only the supercapacitor bank was connected to take advantage of the fast-charging capability. In the experiment of Karandikar, it was observed that more energy was recovered when the supercapacitor was partially charged, compared to when fully drained. Interestingly, in Permana's work, the algorithm used was that when the supercapacitor charge goes below 30%, it gets recharged by the battery up to 80%. So, the source of the supercapacitor charge comes from both regenerative braking and the battery.

E-bikes are historically mainly driven using batteries as battery technology continues to improve, and with the development of supercapacitors, another option became available. But a hybrid combination of battery and supercapacitors can increase the range and efficiency of the e-bike drive (Dash *et al.* 2022).

2.4. Methods of power conversion

During braking, kinetic energy developed by vehicle movement is lost due to friction. Regenerative braking recovers a part of this energy by switching the operation of the motor into a generator, where the kinetic energy is converted to electrical energy, then used to charge the power supply (Naveed *et al.* 2022; Vasiljević *et al* 2022). Regenerative braking in e-bikes is only possible with a direct drive

motor since it does not have a freewheeling mechanism and needs to be continuously engaged (ebikes.ca 2024).

In the work of Balaji, they created a prototype using a mid-drive motor mounted on the pedal, but with the freewheeling mechanism removed, as required in regenerative braking. Figure 3 shows the transmission system used in the prototype. With the gear and chain, the motor rotates at a proportional rate with the wheel when not pedalling. For energy recovery, there were no power conversion circuits, only a switch that connects the motor to a capacitor that charges the battery. Karandikar added an alternator with a rectifier, which converts mechanical into electrical energy. He used the alternator of a Maruti Suzuki 800 (engine displacement is 800cc) with a pulley system connected to the BLDC hub motor of the e-bike. The alternator charges a supercapacitor bank during braking after running the motor to a fixed speed of 21km/h.

Removed due to copyright restrictions.

Figure 3. Model of transmission system using a mid-drive motor (Balaji *et al.* 2011).

The most common used configuration for power conversion of recovered energy was the bidirectional DC-DC converter (BDC). It was implemented by multiple studies [3 - 10]. As the name states, bidirectional DC-DC converters allow conversion of voltage on both directions. Direction of current can be switched as necessary. The non-isolated half-bridge topology shown in figure 4 was found to have high efficiency for both buck and boost modes, while requiring few components (Sharma *et al.* 2018). However, a controller for switching the operation of MOSFETS Q_1 and Q_2 is needed. In the regenerative braking application, the current direction is controlled through an electronic switch in the brake lever. This improves on the design of Balaji, whose study only focused on the generated voltages by the motor at various speeds of the e-bike.

Removed due to copyright restrictions.

Figure 4. Non-isolated half-bridge bidirectional DC-DC converter (Sharma *et al.* 2018).

A typical BLDC motor used in e-bikes has three-phases, with a trapezoidal profile for the back EMF. As shown in the timing diagram in figure 5, at most only two phases are connected at a time. To capture all the energy from the motor, there must be some way of switching between phases that synchronizes with the changes in motor line voltage. Details about the control application of the BDC, however, was not discussed in any of the works.

Removed due to copyright restrictions.

Figure 5. Timing diagram for three-phase motor line voltages (Morchin and Oman 2006).

An alternative form of power conversion was proposed by Naveed, using a three-phase rectifier to capture the voltage at all three phases of the BLDC motor. A three-phase bridge rectifier consists of six diodes conducting 120° each, and in pairs. It does not require any control for synchronization as conduction depends on the position of the motor (Rashid 2014).

Removed due to copyright restrictions.

Figure 6. Three-phase bridge rectifier (Rashid 2014).

2.5. Testing approach

2.5.1. Prototype testing

Two types of approaches were done in testing and analysis of regenerative braking, the first was through prototype testing. Most of the prototypes use in testing were normal bicycles converted into an e-bike by fitting BLDC motors [1-6] [9-11]. All of the studies, except Karandikar's (2012) and Naveed's (2022) used motors above the 250W limit, with the largest rated at 2kW.

A common theme in the studies was how potential for energy recovery increases as the e-bike goes faster. Kinetic energy is calculated using the formula:

$$K_e = \frac{1}{2}mv^2 [J] \quad (3)$$

Balaji *et al.* (2011) used a chassis dynamometer to measure generated voltage at various speeds of the modified bike. Without a load, the voltage generated topped 21V at 40kmh, from a low of 4V at 7kmh. While with a load attached, the measurements were 15 and 3V, respectively. The results of their regenerative braking configuration showed an improvement of the battery discharge by 9.05%. But stopping distance was not considered at all, as the test involved turning on the reg brake until the bike stops by itself. At 45kmh, the stopping time was around 17sec, resulting in a stopping distance of 106.25m, which is impractical.

The system of Karandikar, which used an alternator for the power conversion, and supercapacitor sharing the current load with the battery during starting, measured an increase in the range by 5%. Same as above, the testing used only the electronic brakes (and gravity) until stop, measuring braking distances between 22m and 37m. The authors, however, mentioned that the range was likely to increase with optimum components. Figure 7 shows the load sharing between battery and supercapacitor during motor starting. The supercapacitor provided up to 90% of the current during the first second from starting.

Removed due to copyright restrictions.

Figure 7. Current of battery and supercapacitor when starting the motor (Karandikar 2012).

Malan *et al.* (2014) was successful in their target of travelling the campus route of 1100m at a top speed of 25km/h, with a supercapacitor-only power source. But in addition to the regenerative braking, 3 charging spots were used in the route, that was able to fully charge the supercapacitor bank within 30sec. Though the contribution of regenerative braking was not highlighted, it did however, showed that supercapacitors can provide the power for starting the BLDC motor, aside from its quick charging capability.

Sreehari *et al.* (2020) focused on two features, the regenerative braking and self-balancing assist. The results of the brake section of the paper only mentioned success in boosting the motor output

voltage during braking to a constant charging voltage of 27V, but there were no discussions about the actual improvement in the pedal-assist range. Their finding was that the efficiency of the boost converter was only acceptable (above 50%) when the voltage across the motor was at least 5V, indicating a minimum speed to produce effective charging voltage.

Roshan *et al.* (2021), like Balaji measured the voltage at the motor with varying levels of speed. At the maximum test speed of 53km/h, the regenerative voltage was 35V. But with the same speed of 40km/h as Balaji, the voltage at the motor increased from 21V to approximately 32V. A significant difference is that the prototype of Balaji did not use a direct drive motor and used gears and chain to transmit the wheel's power to the motor. It is assumed that the freewheeling was disabled on the modified bike.

The previous studies modified bikes by attaching a motor and controller. Naveed (2022) used an existing e-bike conversion kit and modified to fit their study. The focus of the study was on the limiting of the current consumption from the motor during braking to avoid overloading. This was done using resistive loads controlled through Arduino. Though the use of supercapacitors for storage of regenerated energy was mentioned in the paper, it was not actually implemented.

2.5.2. Simulation model

Two of the studies used different simulation tools in the analysis of regenerative braking for e-bikes. Permana *et al.* (2018) used PSIM software for the author's simulation, while Ilahi *et al.* (2020) used Multisim.

The simulation results of Ilahi showed that their regenerative braking system could increase the mileage of the e-bike by 11km, from an original value of 75km, for a 14.67% improvement. But the analysis only considered the weight of the bike and the rider. In addition to a riding speed twice that of the legal limit for pedal-assist. The model also only used a single-phase BLDC motor, instead of three-phase.

Permana considered the wind drag, rolling resistance, and acceleration force in the power requirement, in addition to the force due to gravity. The author claimed to recover up to 85.61% of the braking energy depending on the brake current. But there are multiple inconsistencies with the study. First is with the cycling speed, the author set a riding speed of 826.34rpm, when converted to km/h using a 19.1inch diameter wheel, results in a speed of 75km/h, which is too fast for an e-bike. Next point is the kinetic energy only measuring 1637.86J. Considering that the total mass of the e-bike and rider was 80kg, then the average speed should have been 6.40m/s (23km/h). Another was the use of NYCC and UC/ECE drive cycles, which are for light duty vehicles, which does not include e-bikes. It was mentioned that the proposed system was tested for 98000s (27.22hours), and for the NYCC cycle the supercapacitor SoC dropped from an initial charge of 89.216% down to 85.559% (3.657% discharge), while the battery DoD was only at 0.031%.

2.6. Gap statement

Based on the reviewed literatures, there were no clear realistic values for the benefits of regenerative braking in electric bicycles. Majority of the works performed testing using fixed speeds and focused on the value of the back EMF of the motor, not on the actual charging aspect. In addition, limitations for the legal road bike, similar to the one here in Australia, were not considered.

2.7. Contribution

The focus of this research project is to propose a regenerative braking system using supercapacitors as the storage of recovered energy. Parameters that will be used for data analysis will be based on values from past studies applied to an actual cycling route and are within the limitations of a road legal e-bike in Australia. Simulation models will be used to determine the improvement in the drive range due to regenerative braking by comparing with the performance of a conventional e-bike ride on a more practical application.

3. METHODOLOGY

3.1. Introduction

The evaluation of performance of the proposed regenerative braking system was carried out through simulation models created in MATLAB/Simulink. The first step was to determine the input parameters for the simulation model. ANSYS Maxwell software was used to design the 250W three-phase BLDC motor and extract the parameters required for the Simulink model. The load parameters, which determines the restrictive forces on the e-bike, were based on values from previous works. While the braking behaviour and the supercapacitor bank value were determined from initial simulation results. The state of discharge (SoD) of the drive sources was the primary gauge used to determine the improvement in pedal assist range and the supercapacitor utilisation.

3.2. Determining of parameters

3.2.1. BLDC motor

The simulation model of the BLDC motor in MATLAB/Simulink required parameters such as the number of poles, armature phase resistance and inductance, and the back-EMF constant, which were not indicated in commercially-available motor specifications. Due to unavailability of parameters, the next best option was to design the BLDC motor using finite element analysis software, ANSYS Maxwell. The parameters used in the BLDC model creation was based on the journals by M. F. Suwarman *et al* (2023), which studied improving efficiency of 350W outer rotor BLDC motors, and S. V. Patil *et al* (2022) and P. Dusane (2016), whose papers focused on how to design and simulate BLDC motors using the ANSYS Maxwell environment.

The motor designed was rated at 36V and 250W, with an outer rotor position and 40 poles. The motor rated speed was set to 25km/h (201rpm). The result was a motor with a stator phase resistance of 13.12m Ω and inductance of 0.48 μ H, and a back EMF constant of 1.609 Vs/rad. The detailed parameters used in ANSYS can be referred to Appendix A.

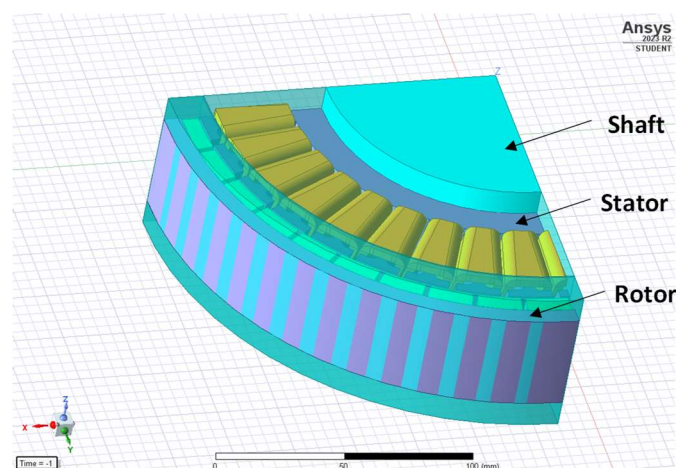


Figure 8. 3D model of the outer rotor BLDC motor used in this study.

3.2.2. Torque load

Another requirement in the creation of the simulation model was to determine the e-bike dynamics, which refers to the forces acting on a bicycle. In order to generate movement, the force of propulsion should be sufficient to overcome the forces restricting the e-bike's movement. For this project, the resistive forces considered include the forces due to gravity (F_g), rolling resistance (F_{rr}), wind drag (F_w), and acceleration (F_a). Based on the book "*Electric Bicycles: A Guide to Design and Use*" by W.C. Morchin and H. Oman (2006), the moment of inertia of the bicycle wheel and components add to the required force for propulsion, but can be assumed negligible in a practical sense, in comparison to the other forces. It is such that it was not considered in this project.

Table 2. E-bike and load parameters

Parameter	Value
Mass of bike and rider (kg)	100
E-bike wheel diameter (mm)	660
Frontal area (m^2)	0.504
Rolling resistance coefficient (C_r)	0.0071
Drag coefficient (C_d)	1
Air density (kg/m^3)	1.225
Wind speed vector (m/s)	0

For the simulations used in this study, it was assumed that the rider and bike have a total mass of 100kg and equipped with 26" (660mm) wheels. The frontal area, which is the surface area perpendicular to the wind, was based on a street-clothed man. Table 2 summarises the load parameters used in the simulation model, for riding in smooth asphalt road and no head wind.

Removed due to copyright restrictions.

Figure 9. Dimensions for a 26" bicycle wheel (bikegremlin.com 2024).

3.2.3. Brake load

Frictional brakes are required to decrease speed of the bicycle. Even with regenerative braking frictional brakes are needed to set the e-bike to a complete stop. To make the model simpler, a controlled torque brake input was used, since the basic function is the same as frictional brakes. In the simulation model, the braking torque load was set as a PWM output with maximum torque of

100Nm. The duty cycle of the PWM was controlled by a PID controller that monitors the actual speed versus the reference defined in the drive cycle.

Table 3. Parameter for torque braking.

Parameter	Value
Maximum brake torque (Nm)	100
Brake torque control used	PWM

3.2.4. Manual pedal input

Peak torque load on a moving body occurs during acceleration, as the torque load is also a function of the acceleration ($Ta = F \times r = ma \times r$). Based on initial observations, peak power required reaches 266W while speeding up at a flat road, exceeding the 250W limit. For road legal e-bikes, manual pedalling is required to activate pedal-assist. Vidal *et al.* (2020) measured pedal torque by cyclists and non-cyclists. Table 4 shows the parameters used for the manual pedal input based on performance of non-cyclist, which benefits more from pedal-assist on non-high-speed applications.

Table 4. Parameters for manual pedal input.

Parameter	Value
Maximum pedal torque (Nm)	32
Pedal cadence (rpm)	70

Some assumptions were made in the manual pedal input in the simulation model:

- Pedalling follows an ideal sinusoidal pattern with minimum at 0Nm.
- Pedalling cadence was assumed constant.
- Pedal peak torque was inversely proportional to the cycling speed.
- Pedal torque was *zero* when riding speed reached maximum speed.

The last item completely removes the pedal torque input at maximum speed and have the e-bike run using battery only. The assumption was that the rider would be mostly freewheeling when the target speed is reached. Since it would only have minimal effects to the battery drain rate, the contribution of pedalling to propulsion was completely removed for constant speed. This also reduced complexity of the simulation model.

Table 5. Drive cycle and riding behaviour parameters used in the test.

Maximum speed (km/h)	25
Maximum speed (rad/s)	21.04
Acceleration (m/s ²)	0.231
Braking deceleration (m/s ²)	3.5
Road inclination - maximum (degrees)	1.09
Road inclination - minimum (degrees)	-0.20
Total drive distance (m)	11,000
Total drive time (s)	1926
No. of stops	23

3.2.5. Drive cycle

The drive cycle represents the riding behaviour of the e-bike user. Table 5 summarises the parameters of the driving behaviour used in this project. The route chosen was a path that passes through a suburb (Pasadena) and the central business district in Adelaide. This represented two types of riding behaviour, mostly long straight drives with few stops, and short drive sections with frequent stops. The route chosen also represented a mostly downhill ride as it was more conducive to regenerative braking. Figures 10 and 11 shows the chosen riding route and the elevation at various sections, respectively. Acceleration was based on the average measurement for 16 cyclists from the study of Parkin and Rotheram (2010), while deceleration due to braking was based on average deceleration rate for calliper and disc brake setup.

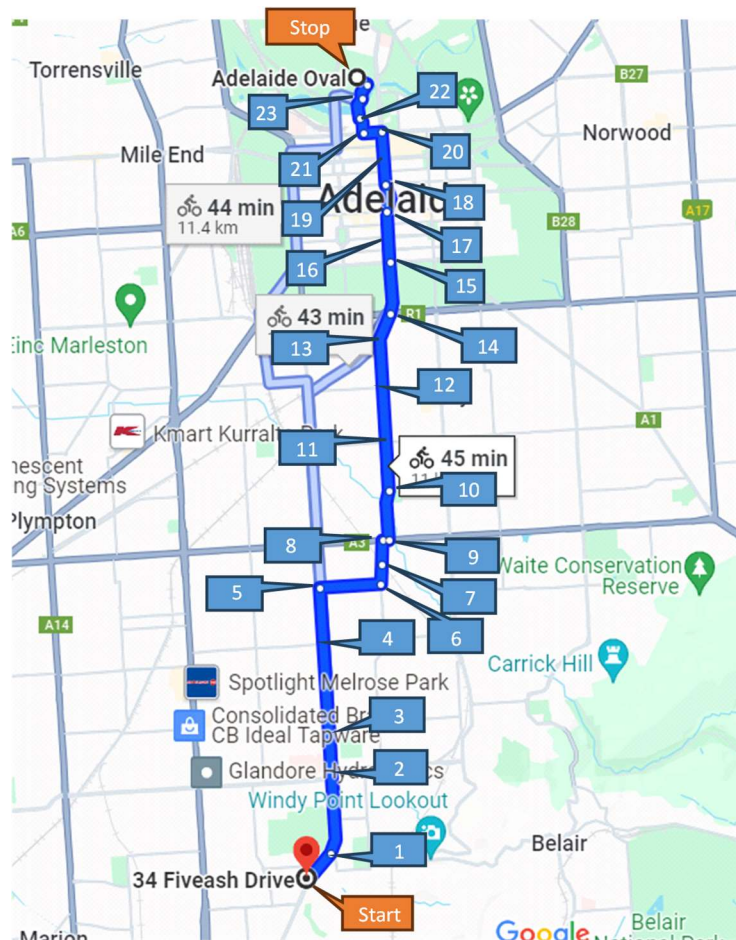


Figure 10. Cycling route used in the drive cycle.

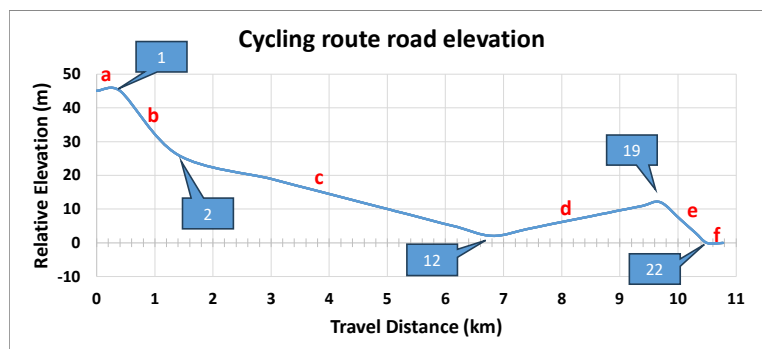


Figure 11. Changes in road elevation at various points of the cycling route.

3.2.6. Battery and supercapacitor

The battery used in the simulation models was a 36V, 418Wh lithium-ion battery, based on the commercially-available BT-E6010 model battery by SHIMANO. While the supercapacitor bank was composed of *ten* 300F, 2.7V supercapacitors connected in series, providing a total rating of 30F, 27V. One of the factors when choosing the supercapacitor was its availability commercially and cost. 2.7V is a common value for supercapacitors. Based on Digikey.com, the cheapest available 300F, 2.7 supercapacitor from Kyocera is AUD14.358, with the next size (400F) can cost between AUD17.920 to AUD36.050. Initial tests also showed that the 30F bank could provide two full acceleration cycles from full charge in a flat road using the load parameters indicated in table 2.

3.3. System model

3.3.1. Conventional e-bike model

The system block diagram for the conventional e-bike model used in this project is illustrated in figure 12. The motor is a three-phase 250W brushless DC motor connected to a three-phase power inverter that outputs trapezoidal voltages similar to the image in figure 4 to produce rotor movement. The inverter output is controlled by a commutation logic that determines the current position of the rotor through the Hall effect sensors. The buck converter adjusts the voltage going to the inverter, and subsequently to the motor, based on the speed requirement. The simulation model used a PID controller that monitors the difference between the drive cycle input reference and the speed sensor measurement. The load to the BLDC motor is in the form of torque, which is a combination of the instantaneous load torque, torque brake, and pedal inputs. The torque brake output is a 100Nm maximum PWM, while the pedal input is represented by a constant frequency with varying peak torque value.

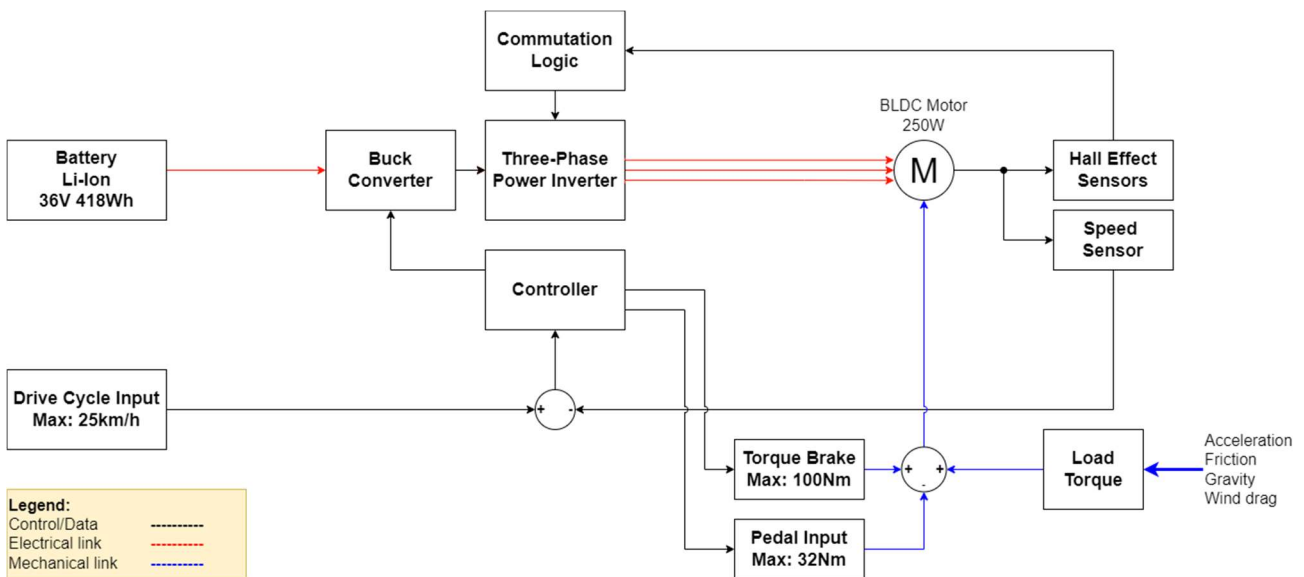


Figure 12. System block diagram of the conventional e-bike model.

3.3.2. Proposed regenerative braking system model

The model for the proposed regenerative braking system added the blocks highlighted in figure 13 below, including additional controller outputs. When power to the motor is cut off during braking, the R-brake switch connected to the motor closes, driving the back EMF through the three-phase bridge rectifier to the 30F, 27V supercapacitor bank. PWM input from the controller to the brake switch controls the braking speed by regulating the back EMF current to the supercapacitor. A boost converter is added that maintains the required voltage to the motor as the supercapacitor charge drops, with an input switch toggling between battery and supercapacitor as main power source.

The simulation model top-level diagram and contents of each block are illustrated in Appendix B.

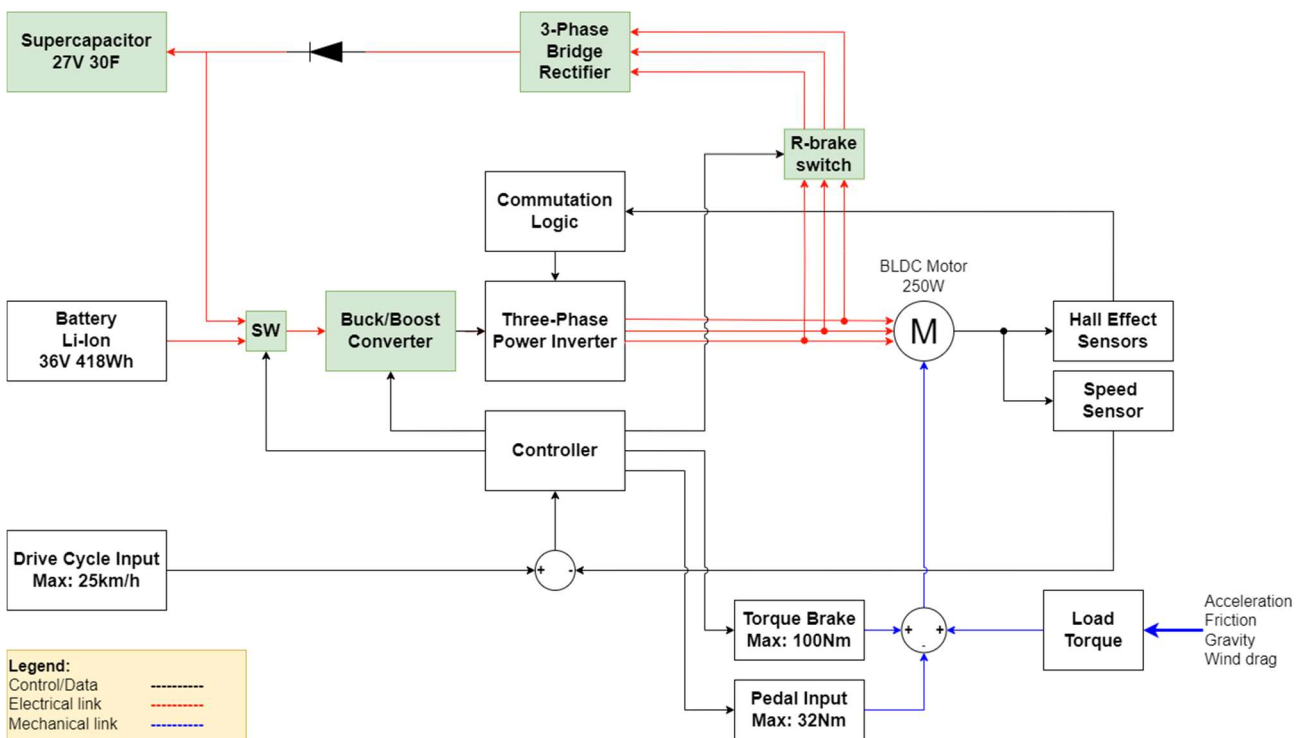


Figure 13. System block diagram of the proposed regenerative braking model.

3.4. Limitations

3.4.1. Data memory and sampling time

The sampling time used in the simulation model was lowered to $10\mu\text{s}$ to improve accuracy of the model. Decreasing the sampling time further down to $1\mu\text{s}$ significantly slowed down the data capture, with the total duration of the drive cycle of 1926 seconds. During data capturing MATLAB crashed several times due to the size of the variable in the workspace became too large for the application and computer to handle (laptop used had 32GB of RAM and available hard drive space above 50GB). To solve this problem, the drive cycle was divided into 9 sections, with the shortest data worth 146 seconds of data (15M data points), and the longest at 247 seconds (25M data points). This was reflected in the final section of the results.

4. RESULTS AND ANALYSIS

4.1. Introduction

This chapter discusses the results and observations from the simulations done in MATLAB/Simulink. The first section focuses on the battery discharge characteristics on an acceleration – constant speed – deceleration cycle. The next part presents the observations on the charging and discharging of supercapacitors subject to changes in road inclination and braking duration. The final part shows the overall improvement in drive range with the derived drive cycle.

4.2. Battery discharge response

The plots in figure 14 illustrates the discharge curve of the battery of an e-bike for one cycle that consisted of a 30 sec acceleration, 41 sec at constant maximum speed, and 2 sec of braking to stop. The battery discharge was exponential during acceleration, then becomes linear with the constant speed. It can be correlated to the additional force required to get the body up to speed. In ideal conditions, once the e-bike reaches the target speed, the required acceleration becomes zero. Peak current consumption occurs during acceleration. Since supercapacitors have high specific power and capable of handling quick bursts of high current, it is more suitable for this state in the drive cycle compared to a battery. But for long and generally stable speeds, switching to battery power is the better option.

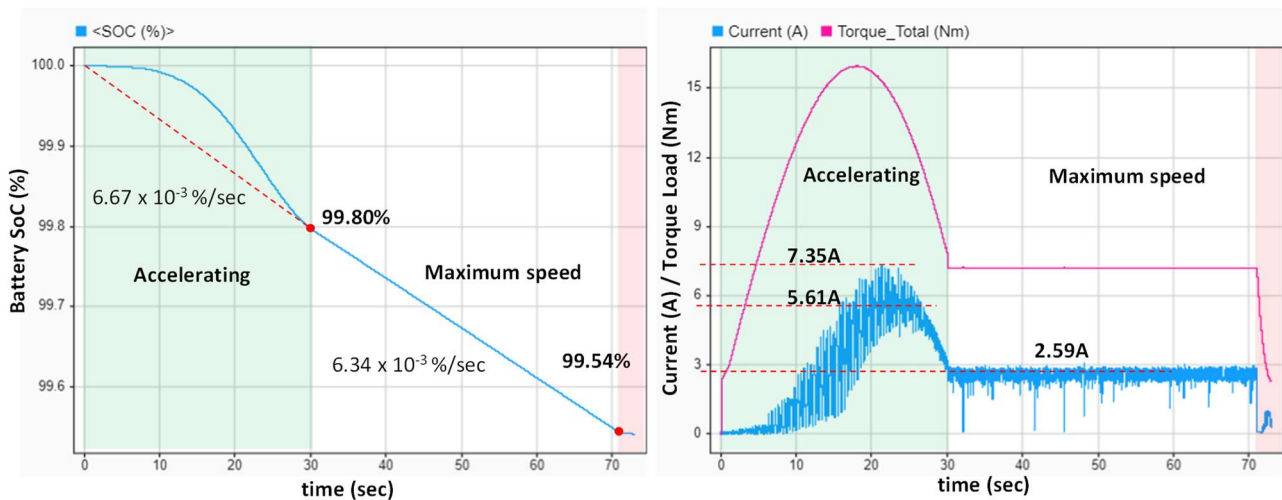


Figure 14. Battery discharge and torque load/current plots for one acceleration-brake cycle.

4.3. Supercapacitor discharging

4.3.1. Discharge characteristics during acceleration

The data in tables 6 and 7 shows the discharging performance of two supercapacitor banks (30F and 15F, respectively) when utilised in the acceleration phase at varying road slopes. For the 30F bank, simulation results show that at a flat road, the supercapacitor can be used for 2 complete

acceleration cycles, then 1 cycle for the steeper 1° and 2° roads. Though it did fail to complete a 1° incline. But at 24.6 sec, the torque load is already decreasing as the acceleration rate decreases near maximum speed. A lower supercapacitor rating of 15F failed to complete the acceleration phase for uphill driver. A higher rating supercapacitor bank of 40F would improve utilization, but as mentioned in the methodology section, components price could increase by at least AUD35.62.

Table 6. Charge of 30F 27V supercapacitor bank after acceleration phase.

Supercapacitor initial charge SoC (%)	Supercapacitor charge after acceleration phase			
	Slope = -1° SoC (%)	Slope = 0° SoC (%)	Slope = 1° SoC (%)	Slope = 2° SoC (%)
99.95	-	80.02	64.42	31.91
70.55	-	25.68	Failed at 24.6sec	Failed at 21.6sec
65.17	45.94	Failed at 28sec	Failed at 22.9sec	-
59.97	38.55	Failed at 25.89s	Failed at 21.2sec	-

Table 7. Charge of 15F 27V supercapacitor bank after acceleration phase.

Supercapacitor initial charge SoC (%)	Supercapacitor charge after acceleration phase			
	Slope = -1° SoC (%)	Slope = 0° SoC (%)	Slope = 1° SoC (%)	Slope = 2° SoC (%)
99.95	79.35	49.58	Failed at 26.14sec	Failed at 22.68sec
70.55	26.10	Failed at 22.68sec	Failed at 19.47sec	Failed at 17.33sec

4.4. Supercapacitor charging characteristics

4.4.1. Charge vs. road slope

The energy recovery performance of the system with varying road elevation is described in table 8. When on a flat road, energy was only recovered during the braking phase (35 sec), with a steeper climb of 1°, the energy recovered was negligible. But with the downhill slope of -1° and -2°, the supercapacitor started charging even before reaching top speed. The brakes were necessary to keep the e-bike within the speed limit. At 0°, only 90.66J, or 3.76% of the total kinetic energy was recovered (2411J).

Table 8. Supercapacitor charge after 1 cycle.

Initial charge	Charge after 1 cycle				Unit
	Slope = -2°	Slope = -1°	Slope = 0°	Slope = 1°	
0.00	26.51	19.80	6.31	0.00	SoC (%)
	8.62	6.66	2.46	0.00	Voltage (V)
Energy recovered	1115.21	665.86	90.66	0.00	Energy (J)

Figure 15 shows the plots of the supercapacitor SoC at different slopes superimposed on the reference speed vs. time graph. As mentioned above, the supercapacitor starts charging before top speed for the downhill rides. Another thing that can be noticed was that charging stopped before the e-bike reached a complete stop. Charging requires the input source to be of higher potential than the storage, and at low speeds the back EMF significantly drops. Charging at low speeds can be possible by introducing a DC-DC boost converter, but this increases system complexity and cost.

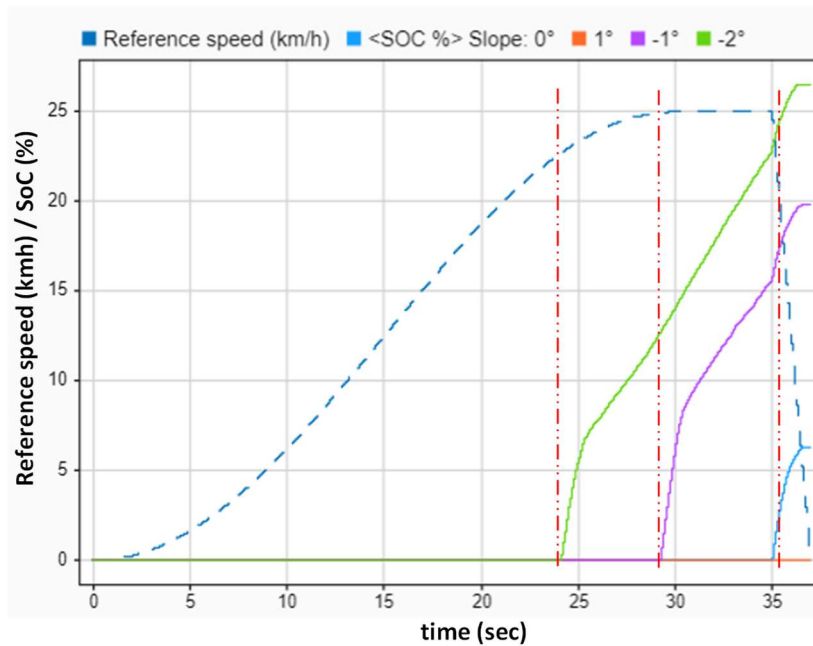


Figure 15. Plot of supercapacitor charge vs. speed and time.

4.4.2. Charge vs. braking distance

Table 9 shows the effect of braking duration to the charging of the supercapacitor. Starting from a hard braking of 1 sec, the brake duration was slowed to a very relaxed 4sec from maximum speed to complete stop. From an initial charge of 0V, the results showed increasing post-brake application charge that peaked with 3.0 sec braking. Longer braking actually caused the potential energy recovery to decline. This was due to the torque loads (wind drag, friction, gravity) become more dominant in slowing down the e-bike at a more relaxed and less steep braking curve.

Table 9. Supercapacitor charge compared to braking distance (slope = 0°).

Braking duration (sec)	Braking distance (m)	Voltage (V)	SoC (%)
1.00	3.47	1.58	3.86
1.50	5.21	2.07	5.19
2.00	6.94	2.40	6.13
2.50	8.68	2.72	7.08
3.00	10.42	3.04	8.04
3.50	12.15	2.63	6.82
4.00	13.89	1.96	4.88

The longer the brake duration, the farther the brake needs to be applied from the target stop. Though there are no specific rules about braking duration, an article on a biking magazine describes the braking distance for a bike decelerating from 25km/h at 7m, which is equivalent to steady braking for 2 sec (rideonmagazine.com.au 2013].

4.5. Drive cycle application

4.5.1. Battery discharge rate

The performance of the battery and supercapacitor performance in the designed drive cycles is shown in table 10 below. As mentioned in the limitations part of the methodology, due to memory limitations, data capture for the drive cycle was divided into 9 sections with varying distances as described in the table.

The road angle highlighted in red indicates a downhill ride, while black refers to a flat or uphill climb. Highlighted blue in the row of the Reg brake data indicates sections where the supercapacitor was utilized (fully or partially) to drive the motor during acceleration phase.

Table 10. Battery and supercapacitor charge status at various sections of the drive cycle.

Item	Drive Cycle section										
	Start	1	2	3	4	5	6	7	8	9	
No. of stops	-	2	1	2	3	2	2	3	4	4	
Drive distance (m)	0	1400	1600	1400	700	1100	1200	1400	1250	950	
Min angle (deg)	-	-1.09	-0.25	-0.25	-0.25	-0.25	-0.25	0.20	-0.86	-0.86	
Max angle (deg)	-	0.00	-0.25	-0.25	-0.25	-0.25	0.20	0.20	0.20	0.00	
No Reg brake	Battery SoC (%)	100.00	99.40	98.26	97.16	96.42	95.51	94.20	92.19	90.69	89.75
	Battery SoC (%)	100.00	99.71	98.81	97.92	97.18	96.28	94.96	92.96	91.46	90.70
w/ Reg brake	SCap SoC (%)	99.95	97.43	72.89	41.80	45.49	47.76	49.33	50.71	65.37	29.10

Figure 16 shows the graphical comparison of the battery of the reference (no regenerative braking) and with application of the proposed system. Immediately, the plot diverges from the start as in the 2nd case, the supercapacitor was used to put the e-bike to speed. The plots continue to separate until the end of the 3rd section when the plots become parallel. At this sections, the charge of the supercapacitor was below the set lower limit (65%). But after the 8th section, which is a downhill of -0.86°, the supercapacitor was able to charge up and be used again at the start of the 9th section.

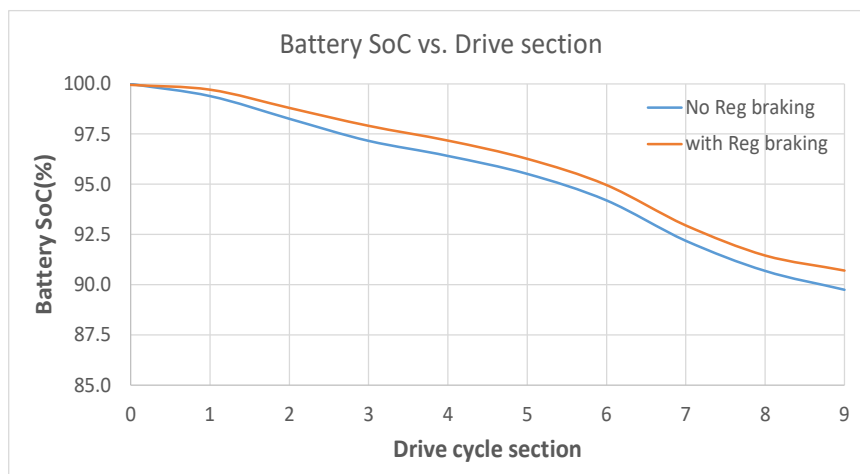


Figure 16. Plot of battery charge at the end of each drive cycle section.

In the case of the reference, the depth of discharge of the battery (DoD) was 10.25% at the end of the drive cycle. While with the proposed system, 9.30% of the charge was used. Using this cycle pattern, the drive range of the motor improved by 10.22%.

4.5.2. Supercapacitor utilisation

Figure 17 gives a graphical representation of the supercapacitor condition at the end of each drive cycle section. Between the end of section 3 and start of section 8, the road angle was between -0.25° and $+0.20^\circ$. And as observed in the results of section 4.3, energy recovery is minimal at flat and incline. In this case, -0.25° was still nearer to flat than -1° . It was only when the downhill slope became steeper at -0.86° that the supercapacitor was able to charge enough to be usable on the next acceleration phase.

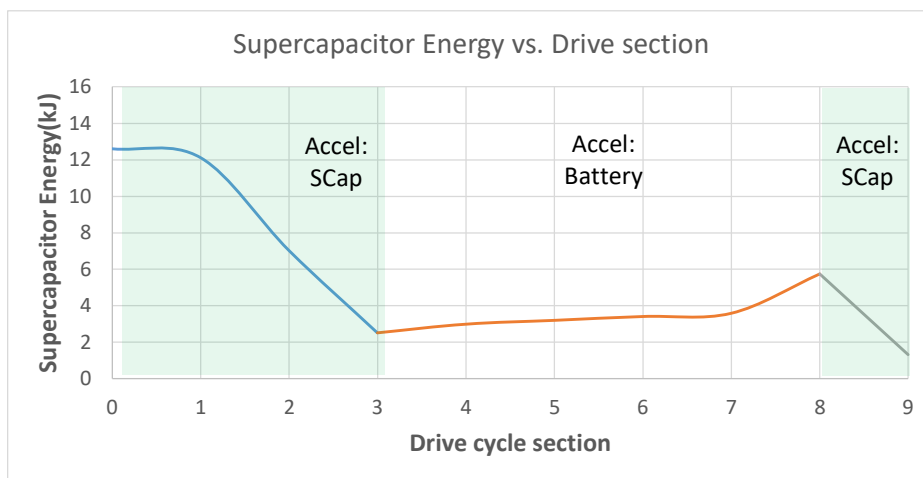


Figure 17. Charge of supercapacitor at the end of each section.

Summarizing the performance of the supercapacitor, it was able to provide the motor a total of 25.20kJ (7.00Wh) of energy, with 1.32kJ (0.36Wh) still remaining at the end of the ride. 13.9kJ (3.86Wh) of energy was recovered during the 23 brake points of the 11km route. With the starting energy of 12.62kJ (3.5Wh), the supercapacitor was able to provide 199.79% of its initial energy. Figure 18 plots the supercapacitor available energy at various points in time of the drive cycle.

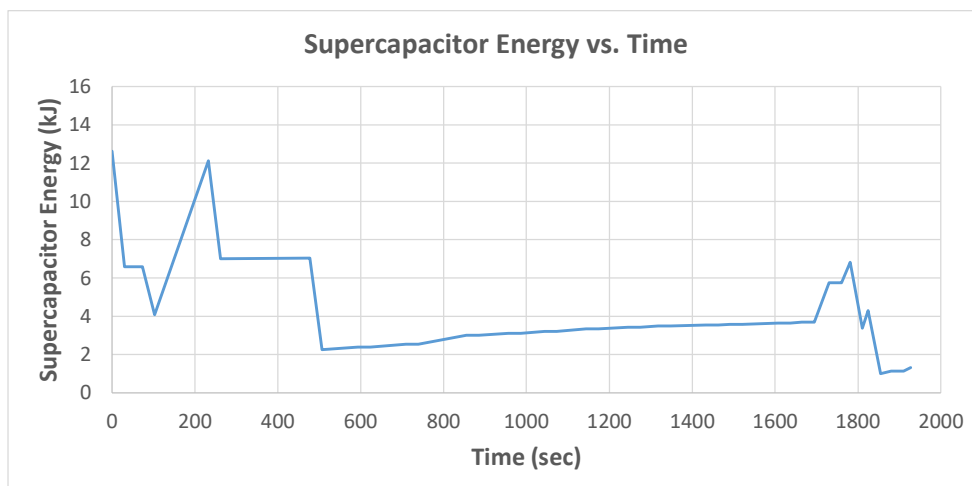


Figure 18. Supercapacitor energy at various points in time.

4.6. Cost comparison

The tables below show the cost comparison of two options for extending the e-bike's drive range. The first option is simply upgrading the battery to the next higher capacity. The second option is the proposed regenerative braking system using supercapacitors. Based only on changes in the hardware, the proposed system would cost about AUD7.76 more than to upgrade the battery to a higher spec.

Table 11. Option 1: Battery upgrade (20% increase in capacity)

Description	Specifications	Price (AUD)	Note
BT-E6010 e-bike battery	418Wh	895.00	Brand: Shimano STEPS series battery Supplier: Melbournepowered.com.au
BT-E8010 e-bike battery	504Wh	1050.00	
	Added cost	155.00	

Table 12. Option 2: Regenerative braking with supercapacitors.

Description	Specifications	Price (AUD)	Note
Supercapacitor (x10)	2.7V, 300F	142.65	Manufacturer number: SCCY62V307VSB Manufacturer: Kyocera AVX
Diode for universal bridge (x6)	100V, 10A	5.88	Manufacturer number: P1000B Manufacturer: Diotec Semiconductor
MOSFET for supercapacitor charging switch	50V, 32A	4.23	Manufacturer number: IXTP32P05T Manufacturer: IXYS
Resistors, Capacitors, and Inductors	-	10.00	
	Total cost	162.76	

5. CONCLUSIONS AND FUTURE WORK

5.1. Conclusions

This project investigated the benefits of a proposed regenerative braking system for e-bikes utilizing supercapacitors as storage for recovered energy. Simulation models of two e-bike systems were developed in Simulink, a conventional pedelec, and one with the proposed regenerative braking system.

As shown in the simulation results, with the limitations in speed, regenerative braking for e-bikes is only effective for downhill rides. The steeper the slope, the less the force opposing movement. At a flat road or an uphill climb, only a small fraction of the energy could potentially be recovered. With the chosen drive cycle route conducive to regenerative braking, the supercapacitor was able to supply the motor almost twice as its initial energy.

In an acceleration to braking cycle, peak current was seen to occur during speeding up. Subjecting the battery to high peak currents can damage the battery or reduce its lifespan. The supercapacitor, with its high specific power, can handle the bursts of high current. The added charge also means less charging cycles for the battery with the same distance travelled. A hybrid system of a supercapacitor and battery that utilizes the former to provide for high currents, can potentially extend the lifespan of the battery.

The results show potential in that the system was able to extend the battery drive range, but there is still much room for improvement to maximize its benefits. One point of improvement is at low riding speed, where the back EMF level drops below the required charging voltage of the supercapacitor. Boosting the back EMF voltage can maximise the energy recovery period during braking. While the proposed regenerative braking system offers a simple solution to extending the drive range, increasing the charging efficiency will require a more complex and expensive system.

As battery technology continues to evolve, prices are expected to get cheaper, which could offset its limited lifespan. And while due to safety reasons, speed and motor output power will continue to be regulated, restricting potential energy recovery. Considering the cost of implementing the regenerative braking system is more expensive than the battery upgrade, a further study that considers battery degradation would be essential in proving if regenerative braking is more beneficial in the long term.

5.2. Future Work

5.2.1. Determination of optimum riding conditions

The simulation results were able to illustrate the potential amount of energy recovery in relation to changes in the input parameters such as the braking distance and the road angle. The possible next step in the study is to determine the optimum riding conditions that will maximise energy recovery. The results will determine the extent that the proposed system can recover energy and ultimately decide if the amount of benefits of the regenerative braking outweigh the increase in cost and complexity of the system.

5.2.2. Improvement of charging efficiency

In the proposed system, another factor that limits the energy recovery is the current charge level of the supercapacitor. Charging is only possible when the potential at the source is higher than the current status of the supercapacitor. Particularly at low speeds, the back EMF of the BLDC motor may not be high enough to surpass the required charging voltage. To maximise the energy recovery is to consider how to raise up the voltage during this stage of the drive cycle while being able to maintain a smooth braking response.

5.2.3. Obtaining more routes and drive cycle data

The drive cycle and route information used in the study was selected partly due to its conduciveness to regenerative braking. But in order to get more comprehensive data on potential energy, more routes and drive cycle data need to be obtained and analysed.

5.2.4. Prototype build and test

It is largely known that simulations have limitations in accuracy but is useful in determining general behaviour of the system with respect to the inputs. In order to validate the results of the simulations, a prototype build and actual road test of the proposed regenerative braking system is required.

BIBLIOGRAPHY

ADIB, A. & DHAOUADI, R. Modeling and analysis of a regenerative braking system with a battery-supercapacitor energy storage. 2017 7th International Conference on Modeling, Simulation, and Applied Optimization (ICMSAO), 4-6 April 2017 2017. 1-6.

BALAJI, SRIDHAR, RAFATH, S. & RANI, J. 2011. Optimized Regenerative Braking Technology For Electric Bikes. *i-Manager's Journal on Mechanical Engineering*, 1, 31-39.

BAYYA, M., RAO, U. M., RAO, B. V. V. S. N. P. & MUTHUKRISHNAN, N. M. Comparison of Voltage Charging Techniques to Increase the Life of Lead Acid Batteries. 2018 IEEE International Symposium on Smart Electronic Systems (iSES) (Formerly iNiS), 17-19 Dec. 2018 2018. 279-284.

BHARATHI SANKAR AMMAIYAPPAN, A. & RAMALINGAM, S. Design, Development and Real-Time Demonstration of Supercapacitor Powered Electric Bicycle. *In: NATHANAIL, E. G., GAVANAS, N. & ADAMOS, G., eds. Smart Energy for Smart Transport, 2023// 2023 Cham. Springer Nature Switzerland*, 125-134.

Bicycle culture (2024) *Wikipedia*. Available at: https://en.wikipedia.org/wiki/Bicycle_culture (Accessed: 24 May 2024).

Consumer sector briefing: E-bikes on the fast track. Available at: <https://www2.deloitte.com/content/dam/Deloitte/de/Documents/consumer-business/Sector-Briefing-E-Bikes-eng.pdf> (Accessed: 24 May 2024).

CONTÒ, C. & BIANCHI, N. 2023. E-Bike Motor Drive: A Review of Configurations and Capabilities. *Energies* [Online], 16.

DUSANE, P. 2016. *Simulation of BLDC Hub Motor in ANSYS - Maxwell*.

FAMIGLIETTI, N. *et al.* (2020) *Bicycle Braking Performance Testing and analysis*, *SAE International Journal of Advances and Current Practices in Mobility*. Available at: <https://www.sae.org/publications/technical-papers/content/2020-01-0876/> (Accessed: 24 May 2024).

Government of South Australia (2023) *Riding a power-assisted bicycle*, *SA.GOV.AU*. Available at: <https://www.sa.gov.au/topics/driving-and-transport/cycling/riding-a-power-assisted-bicycle#:~:text=Road%20rules%20for%20power%20assisted,effective%20brakes> (Accessed: 24 May 2024).

GENC, M. O. 2023. Development of a digital twin model for electric bikes based on urban experimental driving in full electric mode. *Journal of Mechanical Science and Technology*.

GOURISHANKAR, V. and KELLY, D.H. (1973) *Electromechanical Energy Conversion by Vembu Gourishankar and Donald H. Kelly*. New York: Intext Educational Publishers.

HATWAR, N., BISEN, A., DODKE, H., JUNGHARE, A. & KHANAPURKAR, M. Design approach for electric bikes using battery and super capacitor for performance improvement. 16th International IEEE Conference on Intelligent Transportation Systems (ITSC 2013), 6-9 Oct. 2013 2013. 1959-1964.

HE, H. (2022) *Eight disadvantages of electric bikes (do e-bikes have drawbacks?)*, LinkedIn. Available at: <https://www.linkedin.com/pulse/eight-disadvantages-electric-bikesdo-e-bikes-have-drawbacks-holy-he> (Accessed: 24 May 2024).

ILAHI, T., ZAHID, T., ZAHID, M., IQBAL, M., SINDHILA, A. & TAHIR, Q. Design Parameter and Simulation Analysis of Electric Bike Using Bi-Directional Power Converter. 2020 International Conference on Electrical, Communication, and Computer Engineering (ICECCE), 12-13 June 2020 2020. 1-6.

KARANDIKAR, P., TALANGE, D., SARKAR, A., KUMAR, A., SINGH, G. & PAL, R. 2012. Feasibility Study and Implementation of Low Cost Regenerative Braking Scheme in Motorized bicycle Using Supercapacitors. *Journal of Asian Electric Vehicles*, 9.

KUMAR, A., TARNEKAR, D. S. G. & TUTAKNE, D. R. Regenerative Braking Using Super Capacitor in Electric Bike. 2017.

Levin, T. (no date) *The incredible, earth-saving electric bike is having a moment*, Business Insider. Available at: <https://www.businessinsider.com/electric-bikes-popularity-sustainability-evs-2023-4> (Accessed: 24 May 2024).

LIPOWSKY, T., STEGMAIER, J., LANG, M. & LI, P. Simulative potential assessment of regenerative braking with electric bicycles under consideration of realistic boundary conditions. 2017 International Conference on Research and Education in Mechatronics (REM), 14-15 Sept. 2017 2017. 1-7.

LIU, X., LIU, C., LU, M. & LIU, D. Regenerative braking control strategies of switched reluctance machine for electric bicycle. 2008 International Conference on Electrical Machines and Systems, 17-20 Oct. 2008 2008. 3397-3400.

MAIER, O., KRAUSE, M., KRAUTH, S., LANGER, N., PASCHER, P. & WREDE, J. Potential benefit of regenerative braking on electric bicycles. 2016 IEEE International Conference on Advanced Intelligent Mechatronics (AIM), 12-15 July 2016 2016. 1417-1423.

MALAN, K., COUPLAKIS, M. & BRAID, J. Design and development of a prototype super-capacitor powered electric bicycle. 2014 IEEE International Energy Conference (ENERGYCON), 13-16 May 2014 2014. 1434-1439.

Model-based design (no date) *MATLAB & Simulink*. Available at: <https://au.mathworks.com/solutions/model-based-design.html> (Accessed: 24 May 2024).

MOHAMMAD, A., ABEDIN, M. & KHAN, M. Z. 2016. *Implementation of a three phase inverter for BLDC motor drive*.

MORCHIN, W. C. & OMAN, H. 2006. *Electric Bicycles A Guide to Design and Use*, New Jersey, IEEE Press.

MUETZE, A. & TAN, Y. C. Performance evaluation of electric bicycles. Fortieth IAS Annual Meeting. Conference Record of the 2005 Industry Applications Conference, 2005., 2-6 Oct. 2005 2005. 2865-2872 Vol. 4.

NAIN, J., PATRO, K., CHAKRABARTI, A., ROY, R., DAS, B., KASARI, P. R. & BISWAS, S. K. Super Capacitor Based Regenerative Braking in EV. 2021 IEEE Transportation Electrification Conference (ITEC-India), 16-19 Dec. 2021 2021. 1-6.

NAVEED, H., NAGRIAL, M., HELLANY, A. & RIZK, J. Advanced Regenerative Braking System Design and Prototype for an Electric Bicycle. 2022 International Conference on Electrical and Computing Technologies and Applications (ICECTA), 23-25 Nov. 2022 2022. 387-394.

Novović, R. *et al.* (2024) *Bicycle Tyre sizing and dimension standards*, *BikeGremlin*. Available at: <https://bike.bikegremlin.com/285/bicycle-tyre-dimensions/> (Accessed: 25 May 2024).

PARKIN, J. & ROTHERAM, J. 2010. Design speeds and acceleration characteristics of bicycle traffic for use in planning, design and appraisal. *Transport Policy*, 17, 335-341.

PATIL, S. V. & SAXENA, R. "Design & Simulation of Brushless DC Motor Using ANSYS for EV Application". 2022 IEEE International Students' Conference on Electrical, Electronics and Computer Science (SCEECS), 19-20 Feb. 2022 2022. 1-5.

PERMANA, D. A., SHOLAHUDDIN, U., HAMDANI, D. & RACHMILDHA, T. D. Study of Supercapacitor Utilization on Regenerative Braking System: Design and Simulation. 2018 5th International Conference on Electric Vehicular Technology (ICEVT), 30-31 Oct. 2018 2018. 88-94.

Power assisted bicycles, wheeled recreational devices (No date) ... Available at: https://www.police.sa.gov.au/__data/assets/pdf_file/0007/954907/2021-Power-Assisted-Bicycles,-Wheeled-Recreational-Devices-and-Electric-Personal-Transporters-Fact-Sheet.pdf (Accessed: 24 May 2024).

RASHID, M. H., KUMAR, N. & KULKARNI, A. R. 2014. *Power Electronics: Devices, Circuits, and Applications*, Boston, Pearson.

Regen - learn (April 2024) *ebikes.ca*. Available at: <https://ebikes.ca/learn/regen.html> (Accessed: 24 May 2024).

Rideonmag (1970) *Stay or go?*, *RideOn*. Available at: <https://rideonmagazine.com.au/stay-or-go> (Accessed: 24 May 2024).

ROSHAN N., T. I., ZAHID T., ZAHID M., ALI M., AND AWAIS 2021 Q.. Design of HMI Based Digital Electric Bike Using DC/AC Power Converter with Regenerative Feature. *PakJET*, 4, 1-7.

SATHIYAN, P., DANIEL & PRATAP, B. 2018. Effective design and analysis of PEDELeC E-bike using MBD approach. *International Journal of Mechanical Engineering and Technology*, 9, 568-577.

SHARMA, A., MISHRA, R., YADAV, A. K. & PHUKAN, A. Bidirectional DC-DC Converter for Incorporating Regenerative Braking in E-bikes. 2018 International Conference on Electrical, Electronics, Communication, Computer, and Optimization Techniques (ICEECCOT), 14-15 Dec. 2018 2018. 1019-1024.

SMETHURST, P. 2015. Crossings: The Diffusion of Bicycle Culture across Asia and Africa. In: SMETHURST, P. (ed.) *The Bicycle — Towards a Global History*. London: Palgrave Macmillan UK.

SREEHARI, M. D., M, K., P, K., A, V., RAM, M. B. J., I, V. & DHARMANA, M. M. Design and Analysis of E-Bike with Electrical Regeneration and Self-Balancing Assist. 2020 4th International Conference on Trends in Electronics and Informatics (ICOEI)(48184), 15-17 June 2020 2020. 119-124.

SUWARMAN, M. F., KUSUMA, I., FURQANI, J. & RIZQIAWAN, A. Optimization Design to Increase Efficiency of 350 W Outer Rotor Brushless DC Motor for Urban Electric Bicycle. 2023 4th

International Conference on High Voltage Engineering and Power Systems (ICHVEPS), 6-10 Aug. 2023 2023. 533-539.

THEJASREE, G., MANIYERI, R. & KULKAMI, P. 2019. *Modeling and Simulation of a Pedelec*.

USTUN, O., TANC, G., KIVANC, O. C. & TOSUN, G. In pursuit of proper BLDC motor design for electric bicycles. 2016 XXII International Conference on Electrical Machines (ICEM), 4-7 Sept. 2016 2016. 1808-1814.

VASILJEVIĆ, S., ALEKSANDROVIĆ, B., GLIŠOVIĆ, J. & MASLAĆ, M. 2022. Regenerative braking on electric vehicles: working principles and benefits of application. *IOP Conference Series. Materials Science and Engineering*, 1271, 012025.

VIDAL, A., BERTIN, D., DROUOT, F., KRONLAND-MARTINET, R. & BOURDIN, C. 2020. Improving the Pedal Force Effectiveness Using Real-Time Sonification. *IEEE Access*, PP, 1-1.

VISHNU, S., DASH, A., PRAVEENA KRISHNA P, S., ARJUN, M. & JAYALAKSHMI N, S. Hybrid Control Algorithm for BLDC Drive Involving Battery and Supercapacitor in E-bikes. 2022 International Virtual Conference on Power Engineering Computing and Control: Developments in Electric Vehicles and Energy Sector for Sustainable Future (PECCON), 5-6 May 2022 2022. 1-6.

VOORDEN, A. M. V., ELIZONDO, L. M. R., PAAP, G. C., VERBOOMEN, J. & SLUIS, L. V. D. The Application of Super Capacitors to relieve Battery-storage systems in Autonomous Renewable Energy Systems. 2007 IEEE Lausanne Power Tech, 1-5 July 2007 2007. 479-484.

APPENDIX A: ANSYS RMXprt PARAMETERS

The following images shows the settings used in the design of the BLDC motor using ANSYS Maxwell environment (ANSYS Electronics Desktop Student 2023 R2).

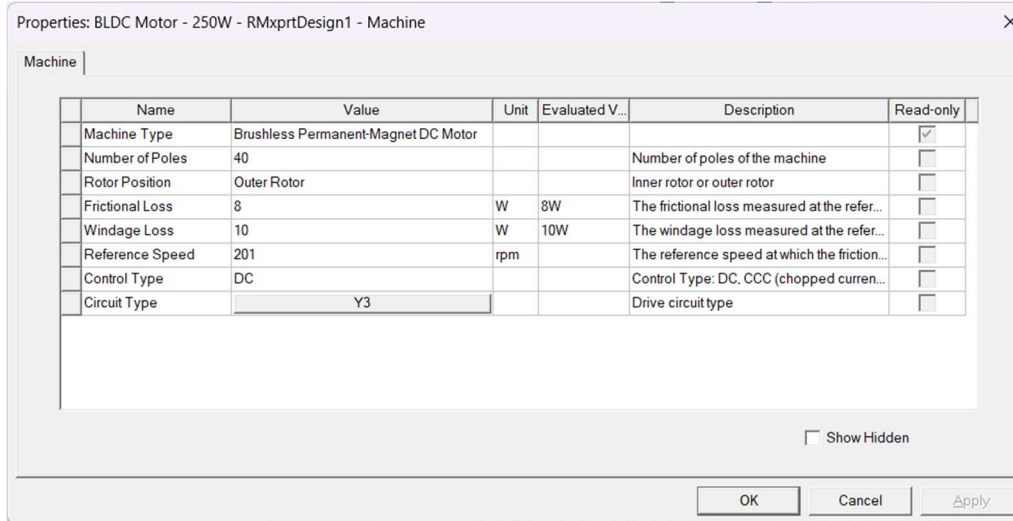


Figure 19. Machine general parameters.

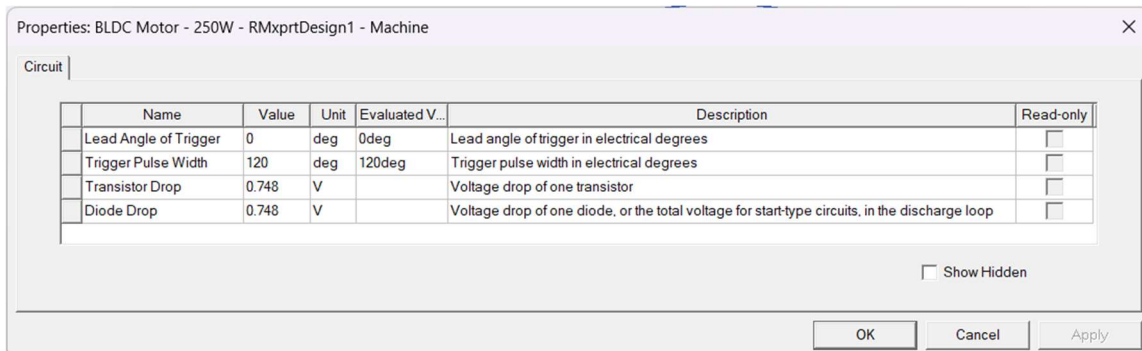


Figure 20. Drive circuit parameters.

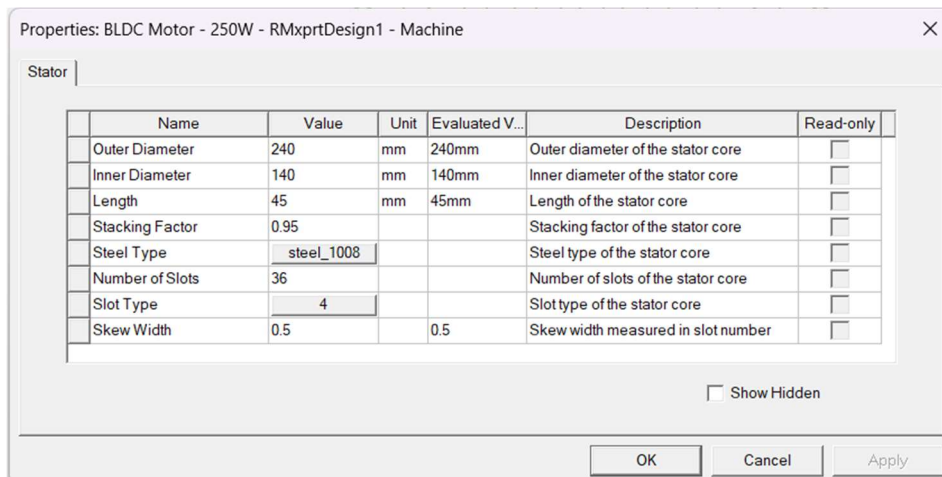


Figure 21. Stator general parameters.

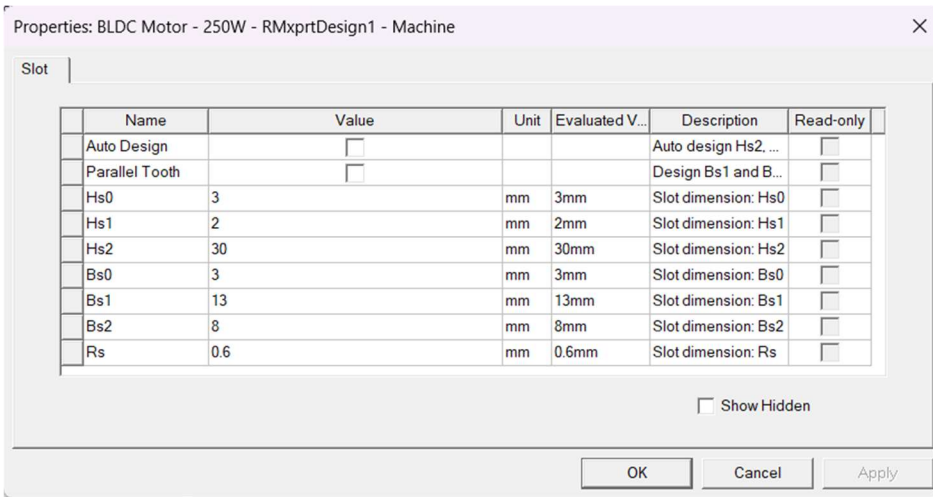


Figure 22. Stator slot dimensions.

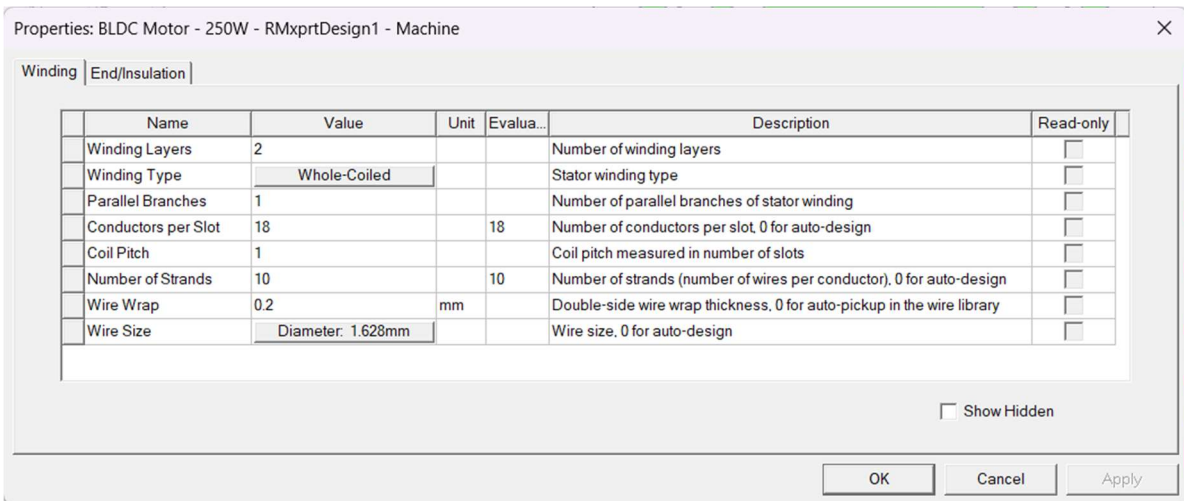


Figure 23. Stator winding parameters.

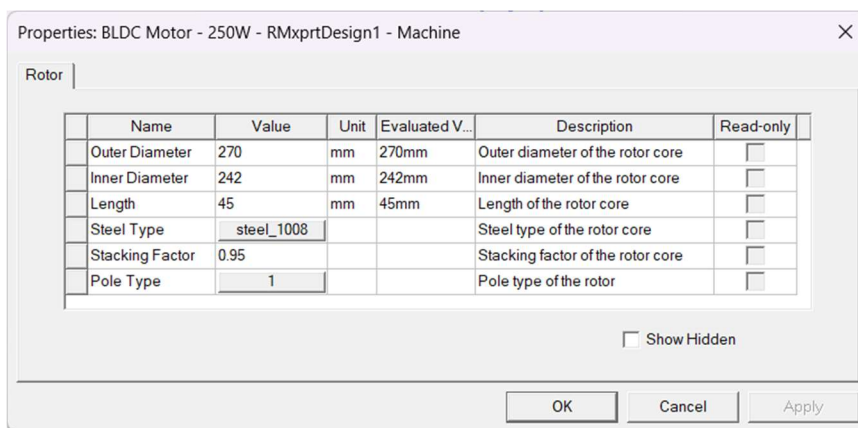


Figure 24. Rotor general parameters.

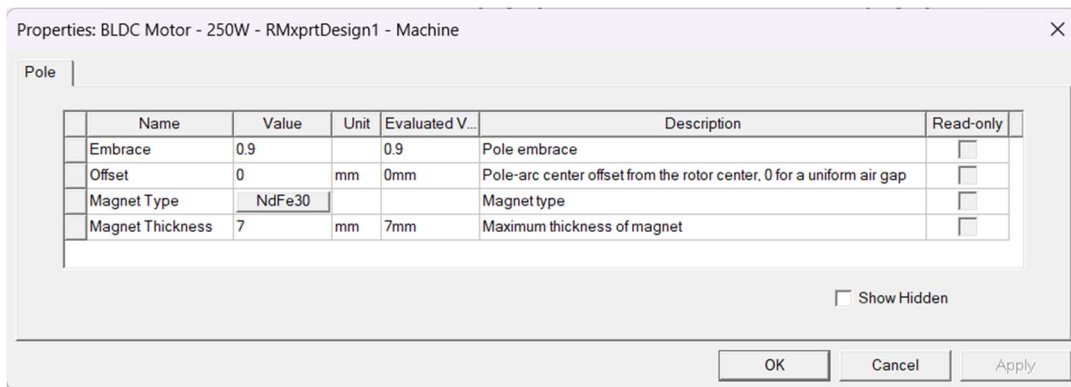


Figure 25. Rotor pole parameters.

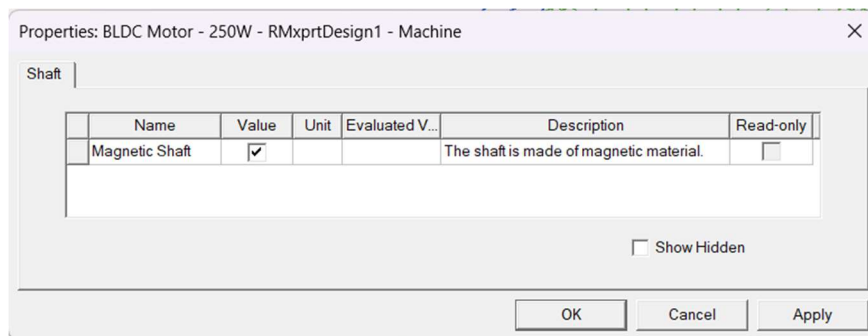


Figure 26. Shaft parameters.

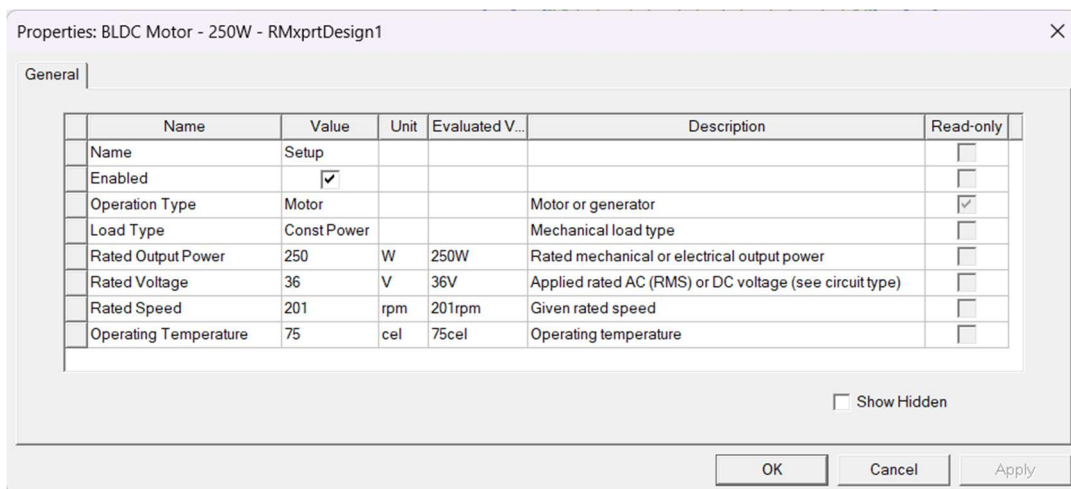


Figure 27. Analysis setup parameters.

APPENDIX B: SIMULATION MODEL BLOCKS

The following images shows regenerative braking simulation model used in this study. Figure 16 shows the top-level of the simulation model.

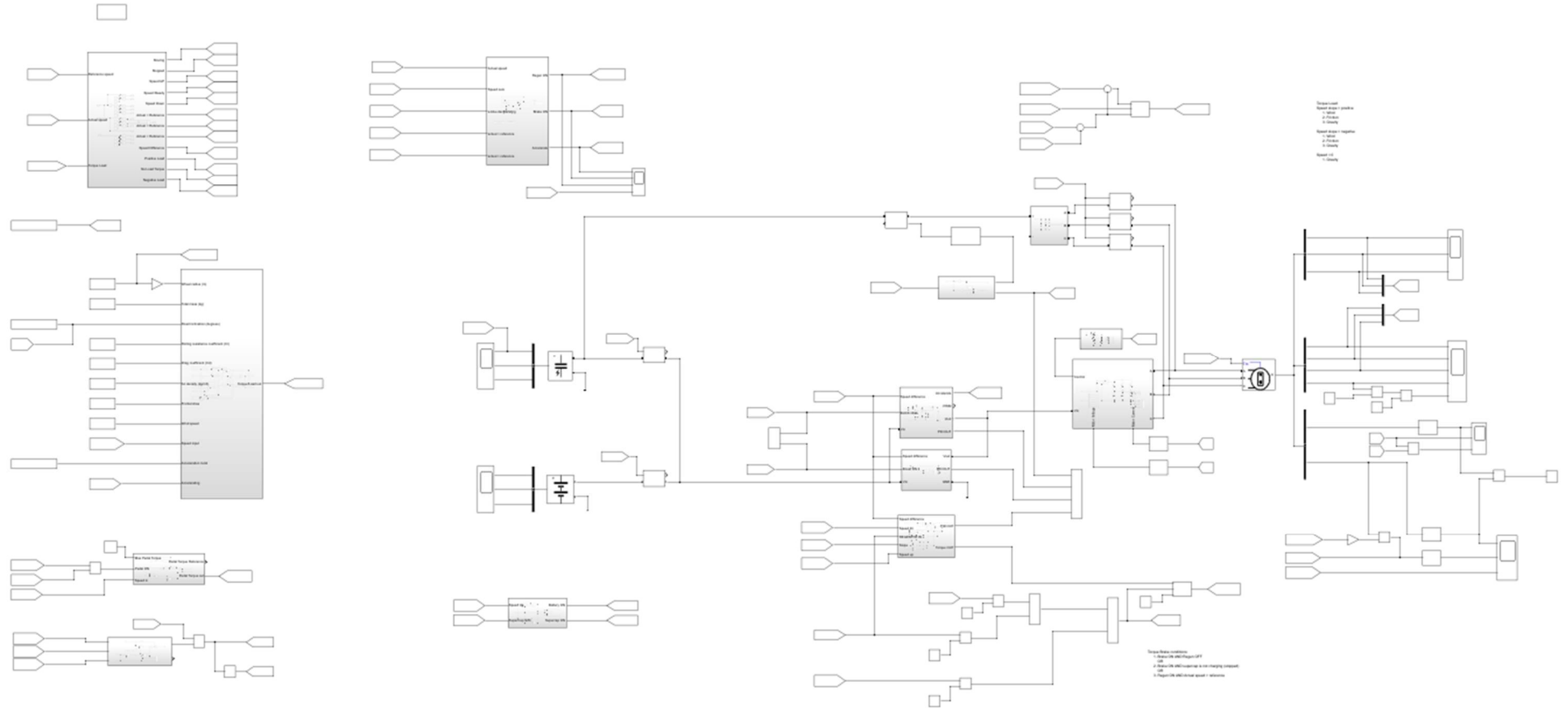


Figure 28. Top-level of Simulink model of Regenerative Braking System.

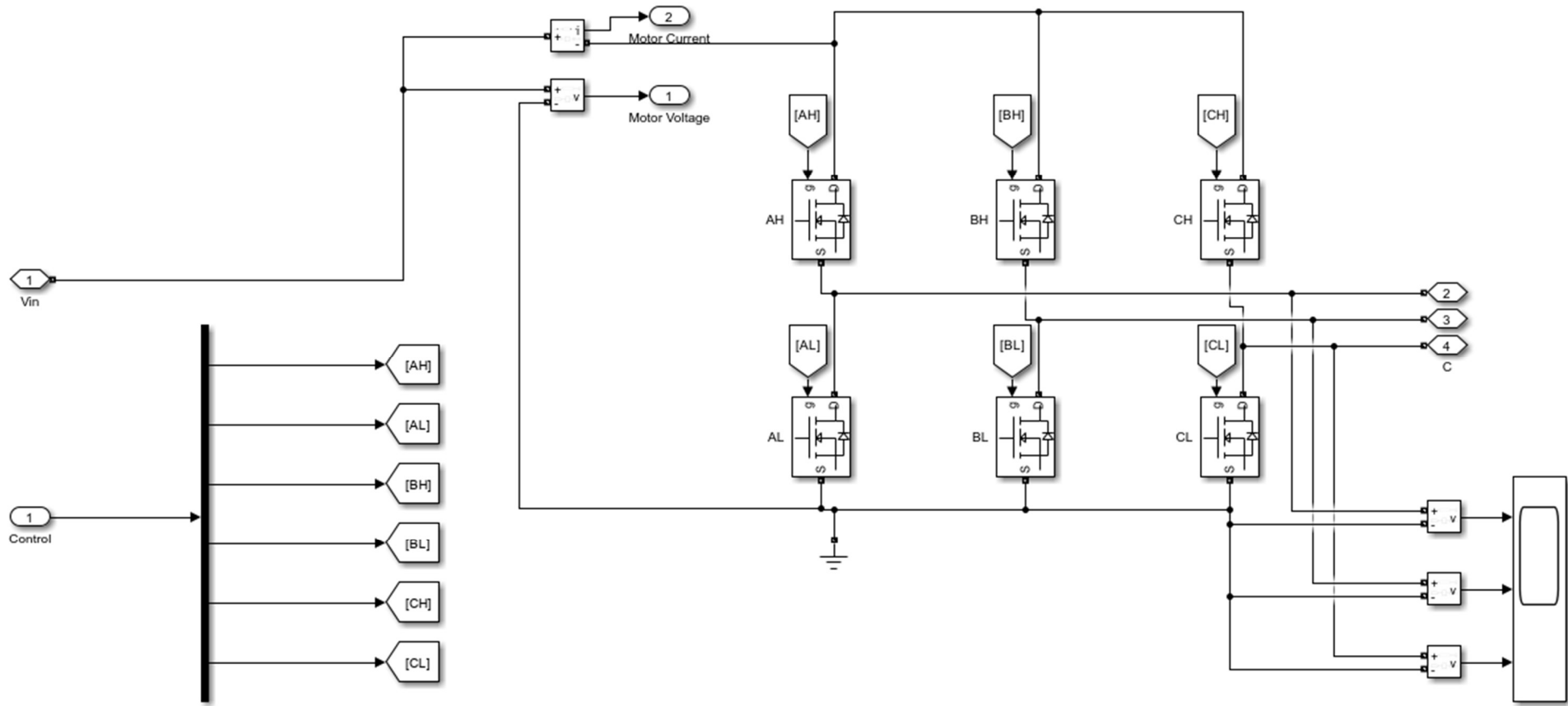


Figure 29. Three-phase power inverter block.

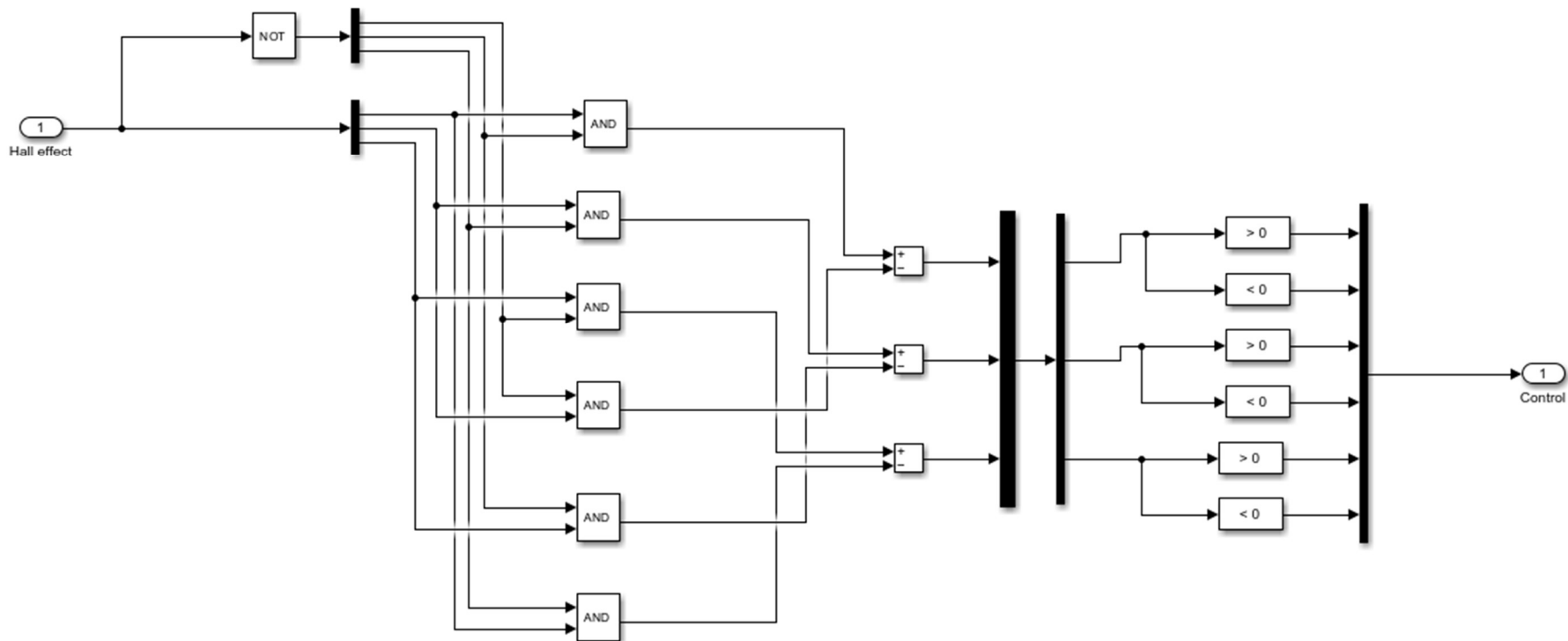


Figure 30. Commutation logic block.

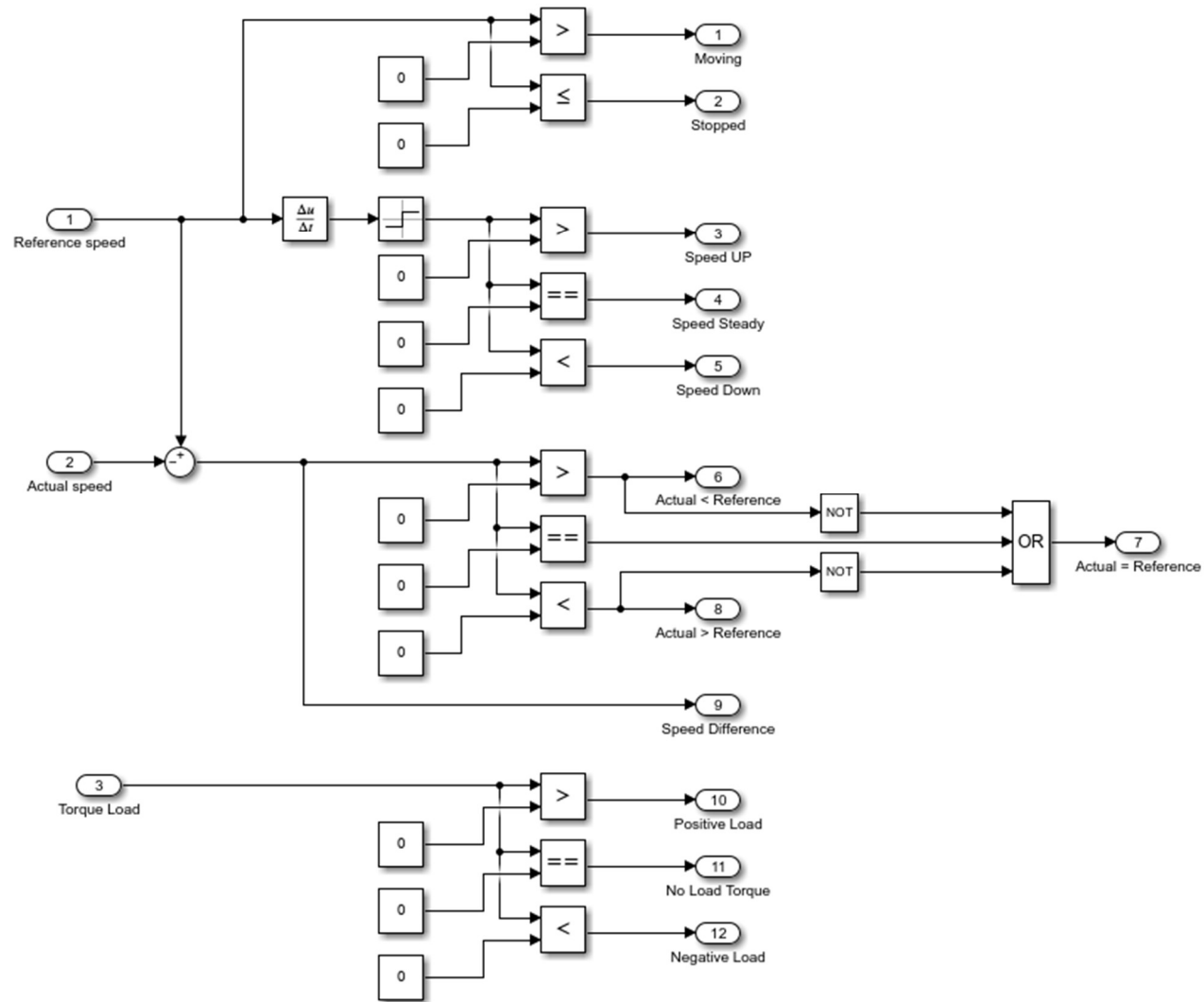


Figure 31. Movement and load status block.

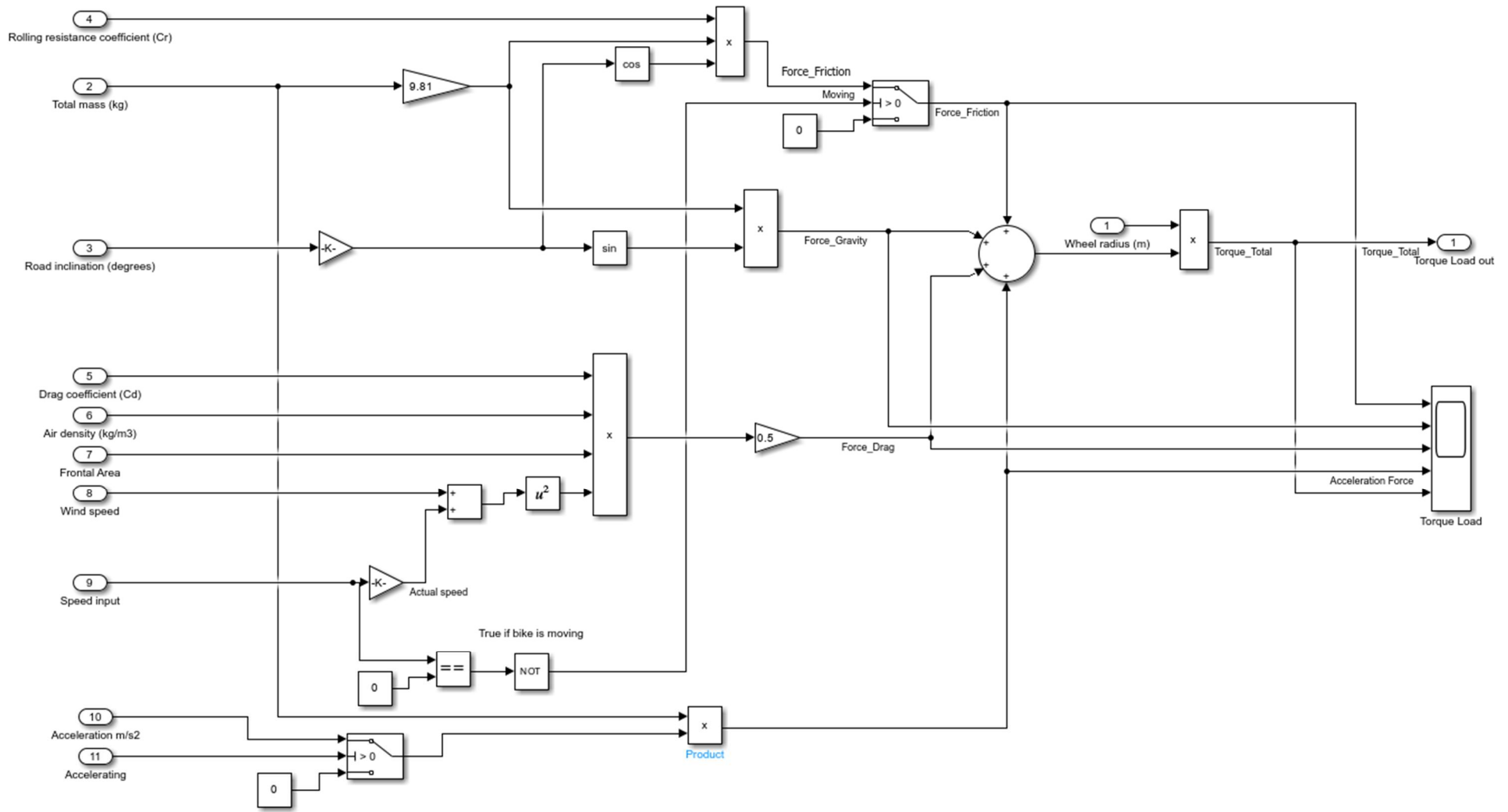


Figure 32. Torque load calculation block.

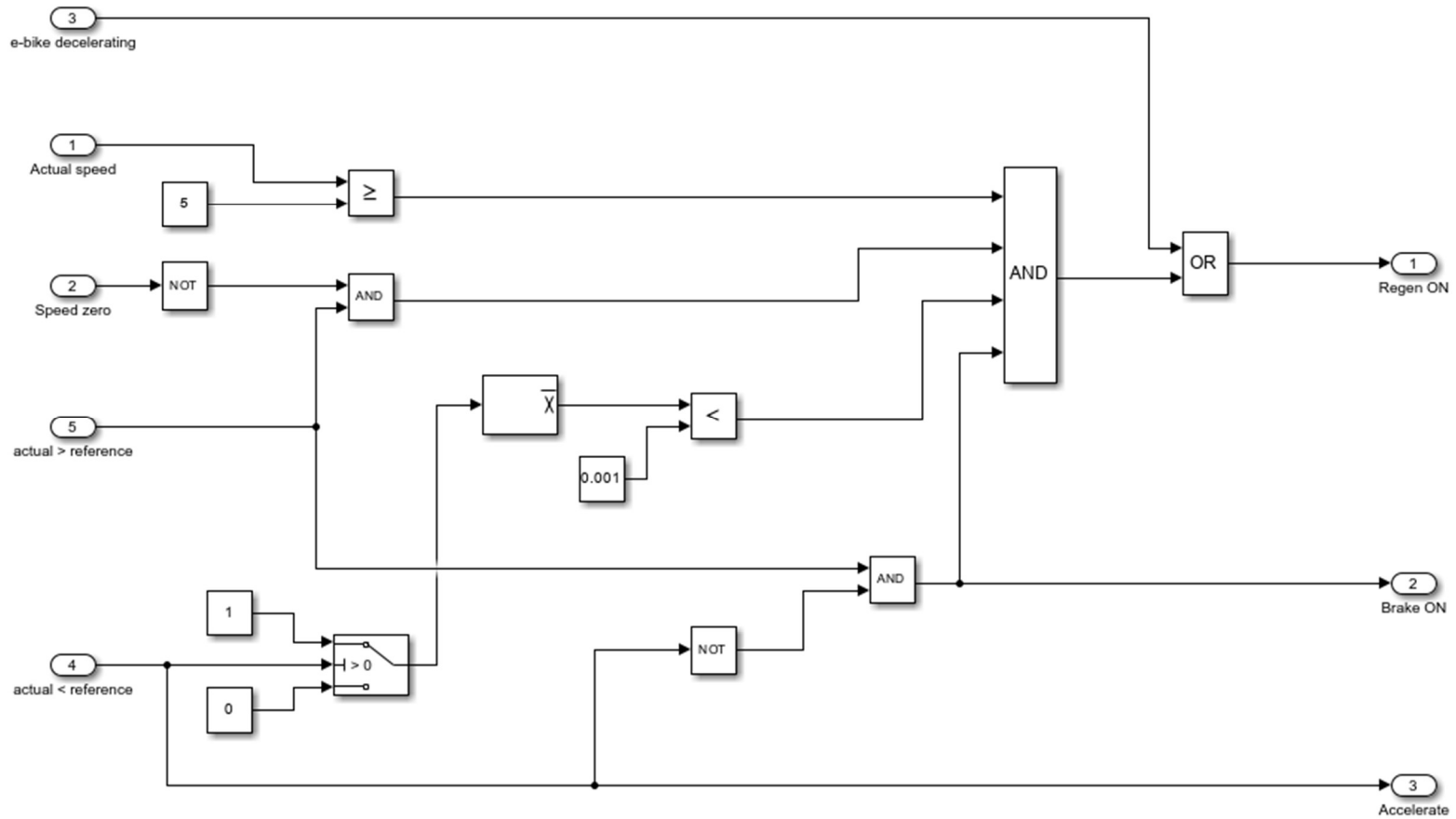


Figure 33. Accelerate/Brake/Regen control block.

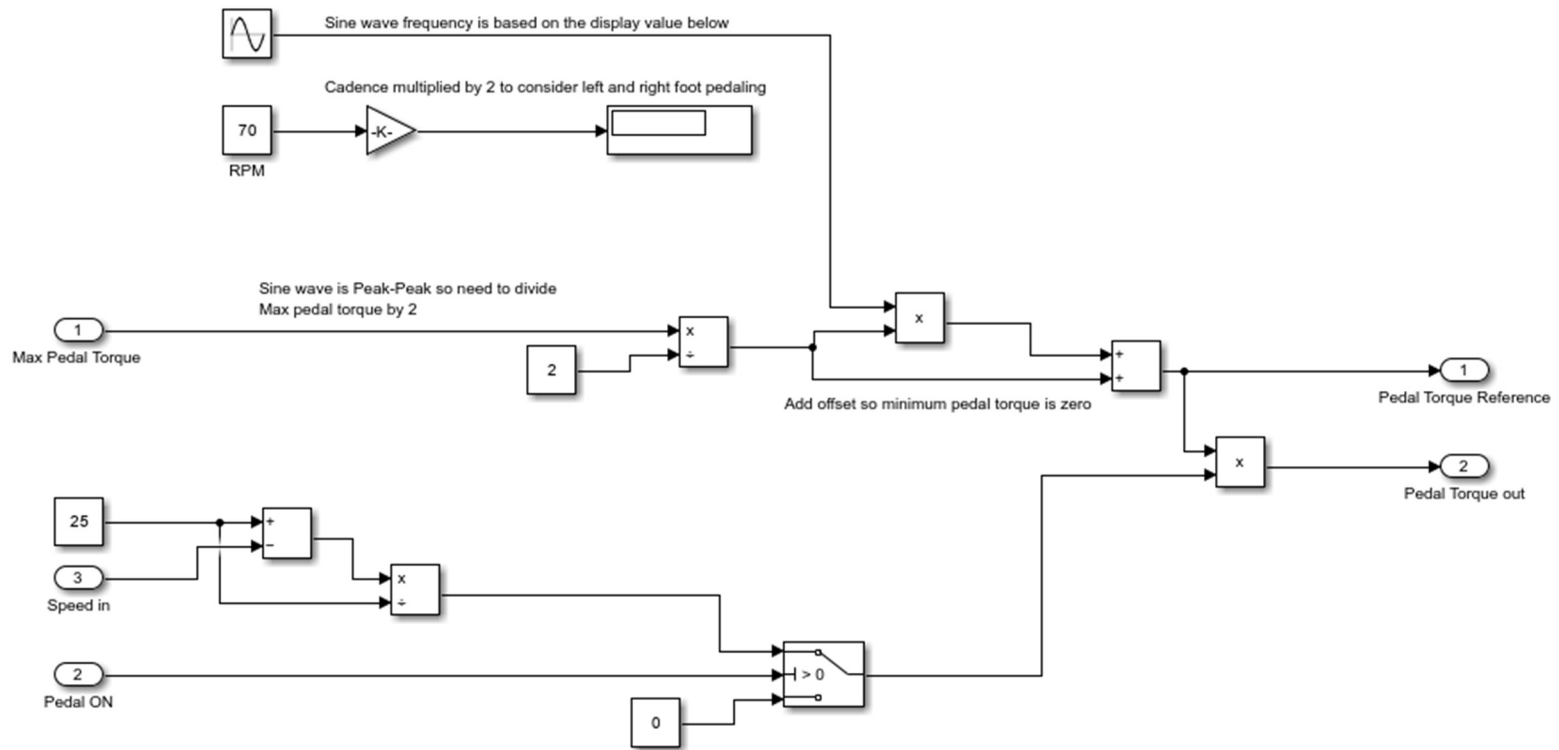


Figure 34. Manual pedal input control block.

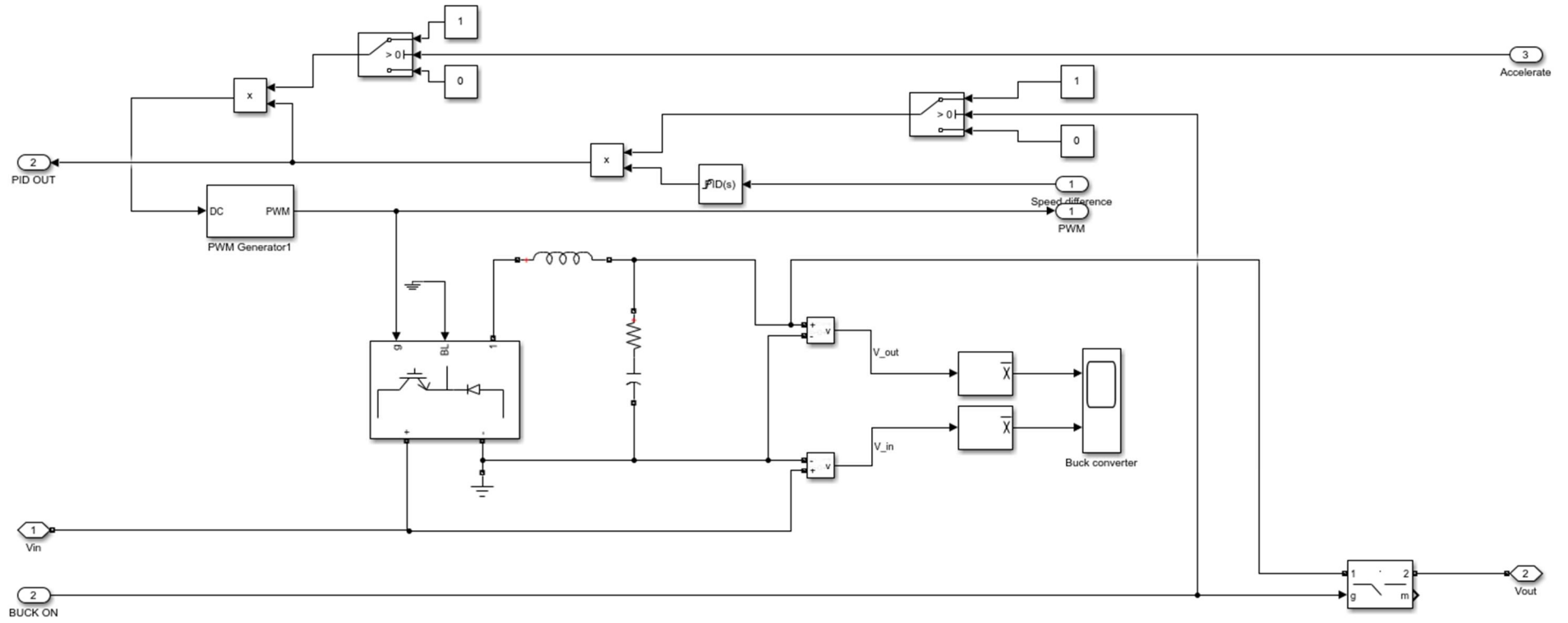


Figure 35. Buck converter block.

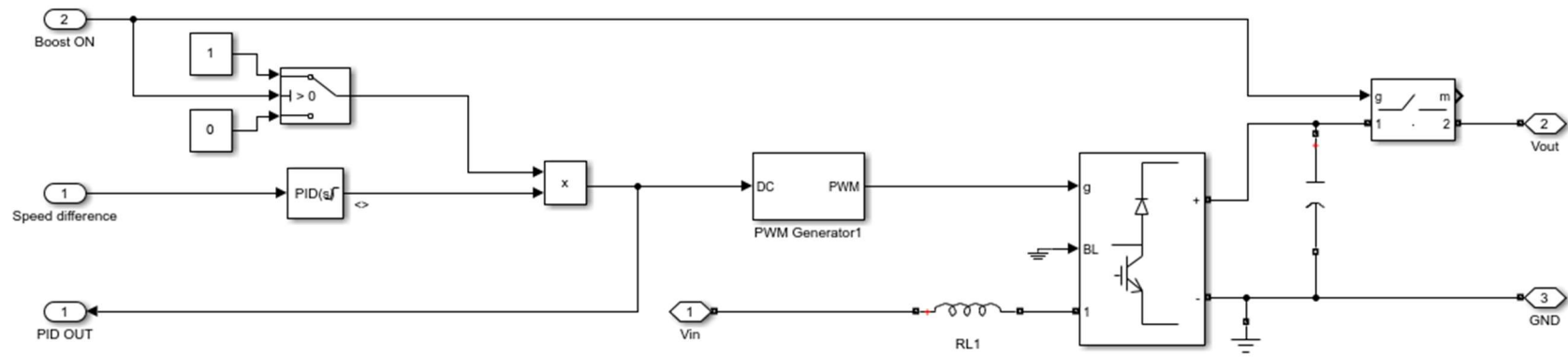


Figure 36. Boost converter block.

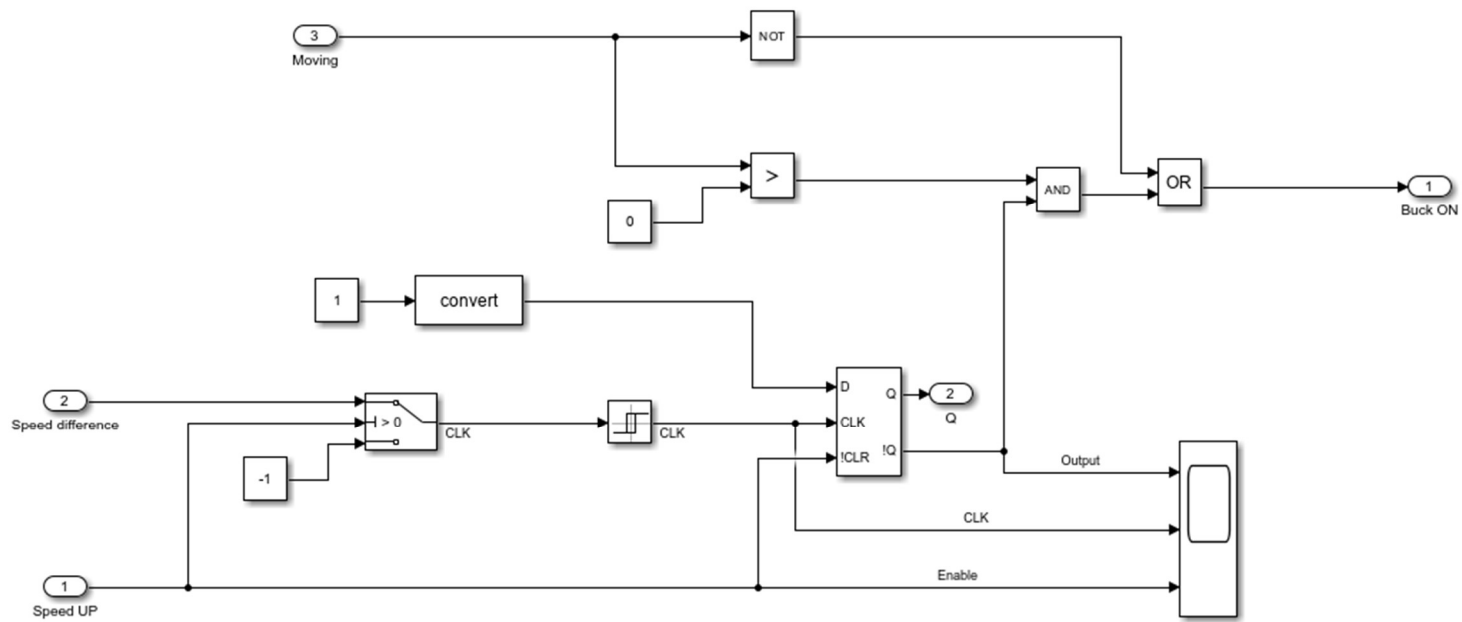


Figure 37. Buck/Boost mode select.

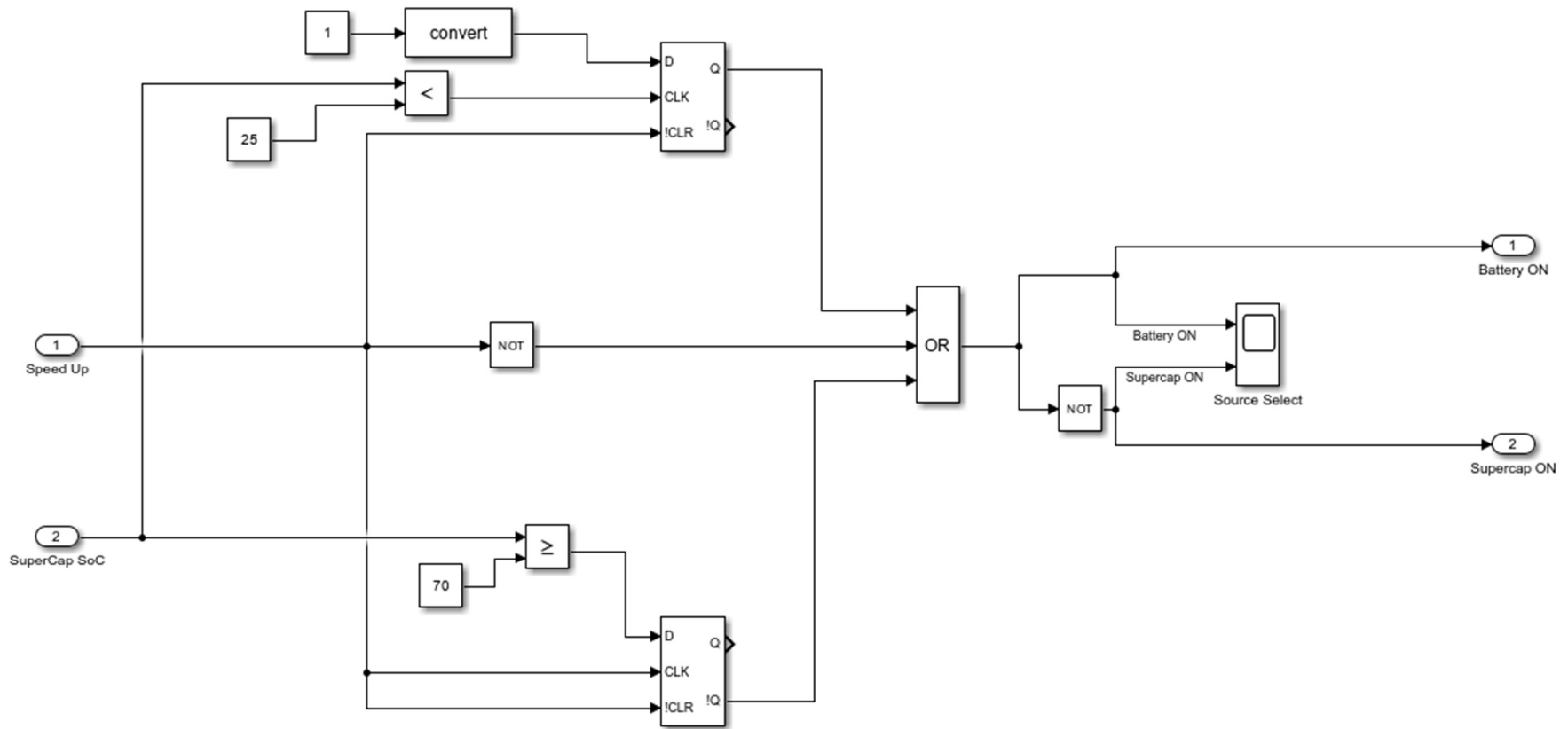


Figure 38. Drive source selection block.

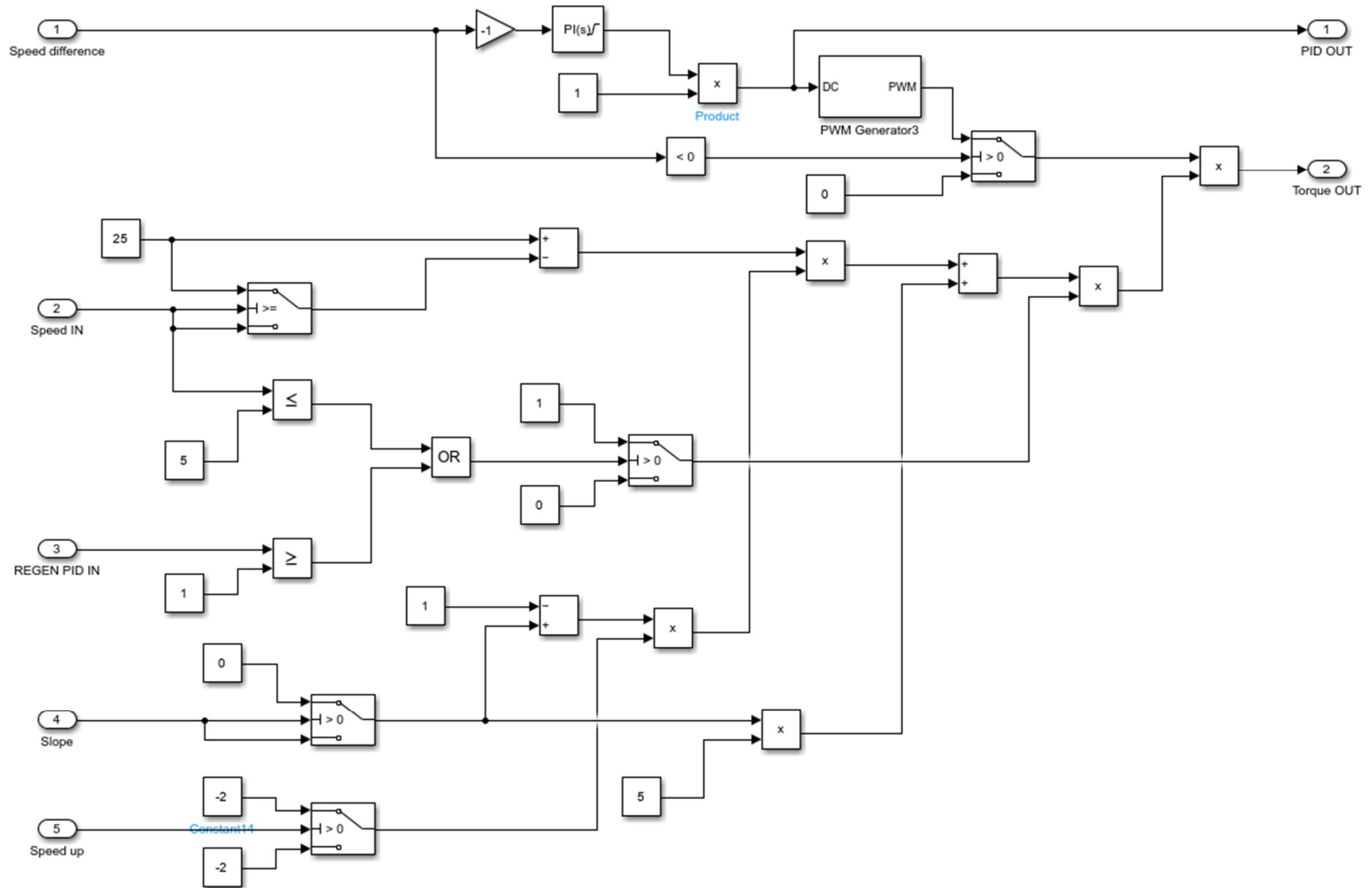


Figure 39. Torque brake controller block.

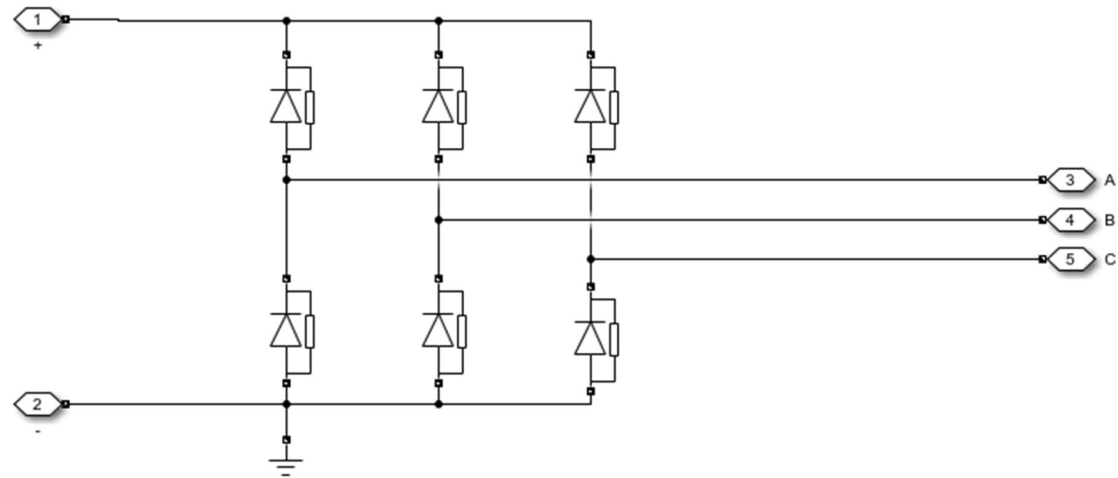


Figure 40. Three-phase bridge rectifier.

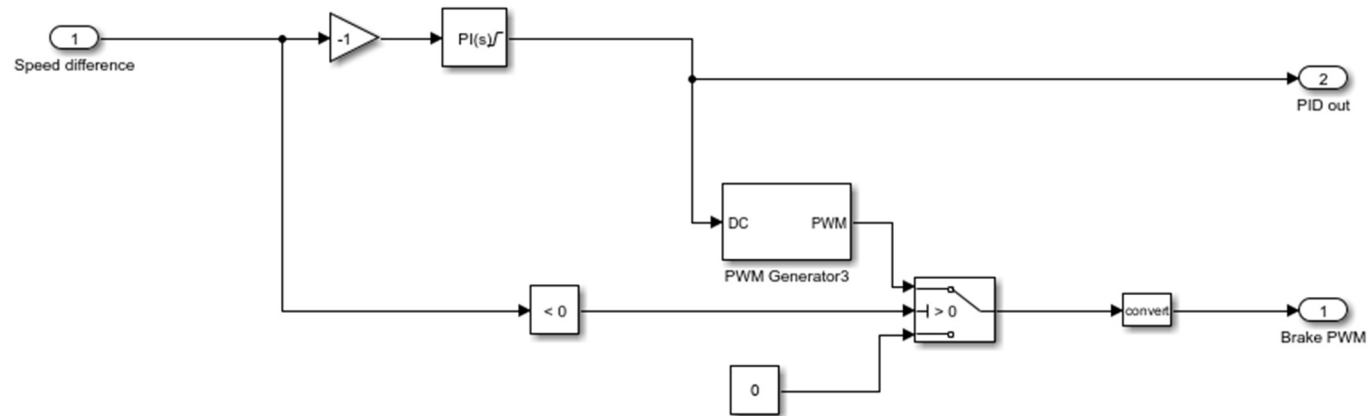


Figure 41. Electronic brake controller.